USTC-ICTS/PCFT-24-12

Dissecting Quantum Many-body Chaos in the Krylov Space

Liangyu Chen,[1] Baoyuan Mu,[1] Huajia Wang,[1,2,*] and Pengfei Zhang[3,4,5,†]

[1] *Kavli Institute for Theoretical Sciences, University of Chinese Academy of Sciences, Beijing 100190, China*
[2] *Peng Huanwu Center for Fundamental Theory, Hefei, Anhui 230026, China.*
[3] *Department of Physics, Fudan University, Shanghai 200438, China*
[4] *Shanghai Qi Zhi Institute, AI Tower, Xuhui District, Shanghai 200232, China*
[5] *Hefei National Laboratory, Hefei, 230088, China*

(Dated: April 15, 2024)

The growth of simple operators is essential for the emergence of chaotic dynamics and quantum thermalization. Recent studies have proposed different measures, including the out-of-time-order correlator and Krylov complexity. It is established that the out-of-time-order correlator serves as the signature of quantum many-body chaos, while the Krylov complexity provides its upper bound. However, there exist non-chaotic systems in which Krylov complexity grows exponentially, indicating that the Krylov complexity itself is not a witness of many-body chaos. In this letter, we introduce the missing ingredient, named as the Krylov metric K_{mn}, which probes the size of the Krylov basis. We propose that the universal criteria for fast scramblers include (i) the exponential growth of Krylov complexity, (ii) the diagonal elements $K_{nn} \sim n^h$ with $h \in (0, 1]$, and (iii) the negligibility of off-diagonal elements K_{mn} with $m \neq n$. We further show that $h = \varkappa/2\alpha$ is a ratio between the quantum Lyapunov exponent $\varkappa$ and the Krylov exponent α. This proposal is supported by both generic arguments and explicit examples, including solvable SYK models, Luttinger Liquids, and many-body localized systems. Our results provide a refined understanding of how chaotic dynamics emerge from the Krylov space perspective.

Introduction.– Understanding how chaotic dynamics emerge and drive systems toward thermal equilibrium is of vital importance in the study of quantum dynamics. It requires encoding all local initial conditions into the entire system after sufficiently long unitary evolutions, a phenomenon known as information scrambling [1, 2]. Inspired by gravity calculations [3–6], the out-of-time-order correlator (OTOC) is introduced as a quantitative measure of quantum many-body chaos [7–11], which provides broad implications in condensed matter physics, quantum information, and high-energy physics. It probes the average operator size, which is a measure of operator complexity in the local basis [11–13]. Of particular interest are chaotic systems with large local Hilbert space dimensions, wherein the OTOC exhibits exponential deviation behavior characterized by quantum Lyapunov exponent $\varkappa$ [8–11, 14]. Examples include the Sachdev-Ye-Kitaev (SYK) model [15–19], Brownian circuits [20–22], and black holes [8, 9, 11, 23], often referred to as fast scramblers [2].

In addition to the OTOC or operator size, various measures of operator complexity have been proposed by selecting different bases [24–32]. The Krylov basis stands out because it provides a convenient and intrinsically defined operator basis generated by the Heisenberg evolution [33–58]. In this basis, the operator dynamics are mapped to the evolution of a wavepacket on a half-infinite chain with nearest-neighbor hopping determined by the Lanczos coefficients b_n. The Krylov complexity $\mathcal{K}(t)$ is then defined as the center-of-mass position at time t. In Ref. [33], it is conjectured that Lanczos coefficients approach a linear form $b_n = \alpha n + \gamma$ at large n for chaotic systems, which gives $\mathcal{K}(t) \propto e^{2\alpha t}$. Furthermore, the Krylov exponent provide an upper bound to the quantum Lyapunov exponent as $\varkappa \leq 2\alpha$ [33, 50], saturated in the large-q SYK model. However, there are instances that exhibit significant discrepancies between the Krylov complexity and the actual chaotic/integrable nature of the system captured by OTOCs. The extreme examples include the Krylov complexity of local operators in a free 2D conformal field theory (CFT) [49], which grows exponentially despite the system being non-interacting.

This naturally leads to the following question: What is the criterion for diagnosing quantum many-body chaos in the

(a)

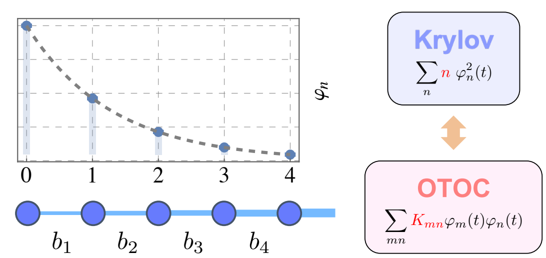

(b)

		b_n	K_{nn}	$K_{mn}(m \ll n)$	Chaotic
SYK+Bath	Scrambling	n	n^h	$\ll \lvert K_{nn}\rvert$	✓
	Dissipative	n	cons.	0	✗
Luttinger Liquid		n	$(-1)^n n^a$	$\sim \lvert K_{nn}\rvert$	✗
MBL Systems		$\sqrt{n}$	$\ln n$	0	✗

FIG. 1. (a). In the Krylov basis, the Heisenberg evolution is mapped to a tight-binding model with nearest neighbor hopping. The Krylov complexity measures the position of the wavepacket, while the equal-time OTOC measures a non-local operator K_{mn}. Here, we assumed the operator $\hat{O}$ is Hermitian. (b). We summarize the results from the SYK models, Luttinger Liquids, and many-body localized systems, which support our criteria.

Krylov space? In this letter, we attempt to elucidate this issue by explicitly representing the OTOC as a non-local observable in the Krylov basis, denoted as a Krylov metric K_{mn}, which measures the size of Krylov basis. The difference between the Krylov complexity and OTOC is then reflected in the distinction between the position operator $n\delta_{mn}$ and K_{mn} for large m and n. We provide the hypothesis for fast scramblers: (i) the Krylov complexity grows exponentially, (ii) the diagonal elements K_{nn} show power-law increase $n^h = n^{\varkappa/2\alpha}$, and (iii) the off-diagonal elements of K_{mn} are negligible. This proposal is supported by examples including the SYK models [15–19], Luttinger Liquids [59], and many-body localized (MBL) systems [60–66], as summarized in FIG. 1.

OTOC in Krylov Space.– The Krylov basis is defined with respect to a simple operator $\hat{O}$ and Hamiltonian $\hat{H}$. Utilizing the operator-state mapping, we express $\hat{O}$ as a state $|O\rangle$ in the doubled Hilbert space. The Heisenberg equation takes the form $d|O\rangle/dt = \mathcal{L}\,|O\rangle$, where $\mathcal{L} := i[H, \cdot]$ denotes the Liouvillian superoperator [67]. The time evolution couples $|O\rangle$ to a set of operators $\{\mathcal{L}^n\,|O\rangle\}$ with $n \in \{0, 1, 2, ...\}$. Applying the Gram-Schmidt procedure with respect to the inner product $\langle O_1|O_2\rangle = \langle O_1^\dagger O_2\rangle = \mathrm{tr}[O_1^\dagger O_2]/\mathrm{tr}[1]$, we obtain the recursive construction for the orthonormal Krylov basis ($n \geq 2$)

$$\begin{aligned} |A_n\rangle &:= \mathcal{L}|O_{n-1}\rangle + b_{n-1}|O_{n-2}\rangle, \\ |O_n\rangle &:= b_n^{-1}|A_n\rangle, \qquad\qquad b_n := \langle A_n|A_n\rangle^{1/2}. \end{aligned} \tag{1}$$

Here, initial conditions are $|O_0\rangle = |O\rangle$ and $|O_1\rangle = b_1^{-1}\mathcal{L}\,|O_0\rangle$. We have assumed that $|O\rangle$ is normalized and b_1 is the normalization factor for $|O_1\rangle$. The set of positive numbers $\{b_n\}$ are called the Lanczos coefficients [68], which only depends on two-point functions $G(t) = \langle O|O(t)\rangle$. Eq. (1) indicates that the Liouvillian superoperator is nearest-neighbour in the Krylov basis. Introducing $\hat{O}(t) = \sum_n \varphi_n(t)\,\hat{O}_n$, the evolution of operator wavefunction $\varphi_n(t)$ is mapped to a tight binding model with $d\varphi_n(t)/dt = b_n\varphi_{n-1}(t) - b_{n+1}\varphi_{n+1}(t)$. The Krylov complexity is defined as the expectation of the position operator $\mathcal{K}(t) := \sum_n n\,|\varphi_n(t)|^2$, which measures how fast the wavepacket spreads towards larger n. Ref. [33] proposed the hypothesis that b_n approaches a linear function $b_n = \alpha n + \gamma$ at large n for chaotic systems in the thermodynamic limit, which results in $\mathcal{K}(t) \sim e^{2\alpha t}$.

We are interested in the relation between Krylov complexity and the OTOC. Our main focus is on its connected part:

$$F(t_1, t_2) = G(t_{12}) \mp \langle \hat{O}(t_2)^\dagger \hat{O}'(0)^\dagger \hat{O}(t_1)\hat{O}'(0)\rangle, \tag{2}$$

where $t_{12} = t_1 - t_2$ and the positive sign is chosen when both $\hat{O}$ and $\hat{O}'$ are fermionic, and we assume the normalization $\langle \hat{O}'^2\rangle = 1$. In chaotic systems with large local Hilbert space dimensions, the OTOC exhibits exponential deviation behavior $F(t_1, t_2) \sim f(t_{12})e^{\varkappa T_{12}}$ with $T_{12} = (t_1 + t_2)/2$ until the scrambling time. It is known that the quantum Lyapunov exponent $\varkappa$ is bounded by the Krylov exponent as $\varkappa \leq 2\alpha$. We rewrite the OTOC by expressing $O(t_i)$ using the operator wavefunction:

$$\begin{aligned} F(t_1, t_2) &= \sum_{mn} K_{mn}\,\varphi_m(t_1)\varphi_n(t_2)^*, \\ K_{mn} &= \delta_{mn} \mp \langle \hat{O}_n^\dagger \hat{O}'(0)^\dagger \hat{O}_m \hat{O}'(0)\rangle. \end{aligned} \tag{3}$$

We refer to K_{mn} as the Krylov metric. Notice that although we focused on the infinite temperature limit in previous discussions, the effects of finite temperature can be incorporated naturally by replacing $\hat{O}$ with $\rho^{\frac{1}{4}}\hat{O}\rho^{\frac{1}{4}}$ [13]. Here, $\rho = e^{-\beta\hat{H}}/\mathrm{tr}[e^{-\beta\hat{H}}]$ is the thermal density matrix. Under this replacement, the two-point function matches the Wightman Green's function $G(t) = \langle \rho^{\frac{1}{2}}\hat{O}(t)\rho^{\frac{1}{2}}\hat{O}\rangle$, and the OTOC exhibits equal imaginary-time separations.

Generic Analysis.– Eq. (3) reveals that the distinction between the OTOC and the Krylov complexity lies in how they measure the Krylov space: The spread of the operator wavefunction depends solely on the Lanczos coefficients, which exhibit an exponential behavior for $b_n \sim \alpha n$. However, this behavior does not necessarily imply quantum many-body chaos for a generic K_{mn}. The manifestation of many-body chaos requires the ability of K_{mn} to measure the spreading in the Krylov space, indicating K_{nn} as an increasing function of n. Physically, as the OTOC measures the growth of operator size in time, the Krylov metric measures the size growth in the Krylov index n. For illustration, let us consider systems that consist of Majorana fermions $\hat{\chi}_j$ with $\{\hat{\chi}_j, \hat{\chi}_k\} = 2\delta_{jk}$. Choosing $\hat{O}' = \hat{\chi}_j$, Eq. (3) becomes [12, 13]

$$\overline{K_{nn}} = \frac{1}{2N}\sum_j \left\langle \left|[\hat{O}_n, \hat{\chi}_j]\right|^2 \right\rangle = \frac{1}{2N}\mathrm{Size}[\hat{O}_n]. \tag{4}$$

Here, we averaged K_{nn} over different j, which is unnecessary for SYK-like models with permutation symmetry between different Majorana modes. Similarly, off-diagonal components K_{mn} measure the interference between $\hat{O}_m$ and $\hat{O}_n$ weighted by the operator size. It is also straightforward to generalize this relation to spin systems [69].

To further motivate the criteria for chaotic systems with exponentially growing OTOC, let's employ a naive scaling argument. Firstly, since $\varkappa$ is bounded by α, a non-vanishing $\varkappa$ requires exponential growth of $\mathcal{K}(t)$. In this scenario, the Krylov complexity suggests the identification $n \sim e^{2\alpha t}$. Applying this relation to the OTOC, we find $F(t, t) \sim e^{\varkappa t} \sim n^h \sim K_{nn}$. Additionally, the validity of this argument necessitates the Krylov metric to be approximately diagonal, i.e., $|K_{mn}| \ll |K_{mm}|$ for $m \gg n$. Otherwise, the double summation in (3) leads to additional enhancement due to off-diagonal coherence. Physically, this occurs because operators with different Krylov indices have different typical sizes, thus their overlap is significantly smaller than diagonal elements. This leads to our universal fast scrambler hypothesis

1. The Lanczos coefficients approach a linear function $b_n = \alpha n$, allowing the Krylov complexity to grow exponentially.

2. The diagonal elements K_{nn} are proportional to n^h, allowing it to measure the spreading in the Krylov space.

3. The off-diagonal elements K_{mn} ($m \neq n$) are negligible, allowing the scaling argument to hold.

Example 1: The SYK Model.– To support our proposal, we first study the Krylov metric in the SYK model [15–19]. In order to achieve a tunable quantum Lyapunov exponent, we couple system fermions, denoted as $\hat{\chi}_j$ ($j = 1, 2, ..., N$), to a series of bath fermions, denoted as $\hat{\psi}_a$ ($a = 1, 2, ..., M$) with $M \gg N$ [70, 71]. The Hamiltonian reads

$$H = \sum_{i<j<k<l} J_{ijkl}\hat{\chi}_i\hat{\chi}_j\hat{\chi}_k\hat{\chi}_l + \sum_{a<b<c<d} J'_{abcd}\hat{\psi}_a\hat{\psi}_b\hat{\psi}_c\hat{\psi}_d + \sum_{i<j}\sum_{a<b} u_{ijab}\hat{\chi}_i\hat{\chi}_j\hat{\psi}_a\hat{\psi}_b. \tag{5}$$

Here, the coupling strengths J_{ijkl}, J'_{abcd}, and u_{ijab} are independent Gaussian varibles with zero means and

$$\overline{J_{ijkl}^2} = \frac{6J^2}{N^3}, \qquad \overline{J'^2_{abcd}} = \frac{6J^2}{M^3} \qquad \overline{u_{ijab}^2} = \frac{2u^2}{NM^2}. \tag{6}$$

The model has been analyzed using the large-N expansion in the low-energy limit with $\beta J \gg 1$ [70]. The (normalized) two-point function for $\hat{O} \sim \hat{\chi}_1$ is given by $G(t) = (\cosh(\alpha t))^{-2\Delta}$, with $\alpha = \pi/\beta$ and $\Delta = 1/4$. Models with a generic Δ can be constructed following a similar strategy. Importantly, the two-point function remains independent of the dimensionless system-bath coupling u/J. Therefore, the Lanczos coefficients and the operator wavefunction match those of the traditional SYK model, which read [33, 48]

$$b_n = \alpha\sqrt{n(n+2\Delta-1)}, \qquad \varphi_n(t) = D_n\frac{\tanh(\alpha t)^n}{\cosh(\alpha t)^{2\Delta}}, \tag{7}$$

where $D_n = \sqrt{\frac{\Gamma(2\Delta+n)}{\Gamma(n+1)\Gamma(2\Delta)}}$. This identifies α as the Krylov exponent. The OTOC with $\hat{O}' \sim \hat{\chi}_2$ can be computed by summing up ladder diagrams [17]. The result reads

$$F(t_1, t_2) = f(t_{12})e^{\varkappa T_{12}} = C_0\frac{e^{2\alpha h T_{12}}}{\cosh(\alpha t_{12})^{2\Delta+h}}, \tag{8}$$

where the Lyapunov exponent $\varkappa = 2h\alpha$ exhibits explicit u/J dependence through $h = \left(1 - \frac{\sqrt{k^4+4k^2}-k^2}{2}\right)$ with $k = u^2/J^2$ [70]. Particularly, in the limit as $k \to \infty$, the Lyapunov exponent $\varkappa \to 0$, indicating the system transitions into a non-chaotic dissipative phase [71].

We explore the origin of the discrepancy between $\varkappa$ and 2α by computing the Krylov metric K_{mn}. Utilizing the analytical knowledge of both the OTOC and the operator wavefunction, we introduce the auxiliary variable $y_i = \tanh(\alpha t_i)$:

$$\left[\prod_i \cosh(\alpha t_i)^{2\Delta}\right] F(t_1, t_2) = C_0\frac{(1+y_1)^h(1+y_2)^h}{(1-y_1y_2)^{2\Delta+h}}. \tag{9}$$

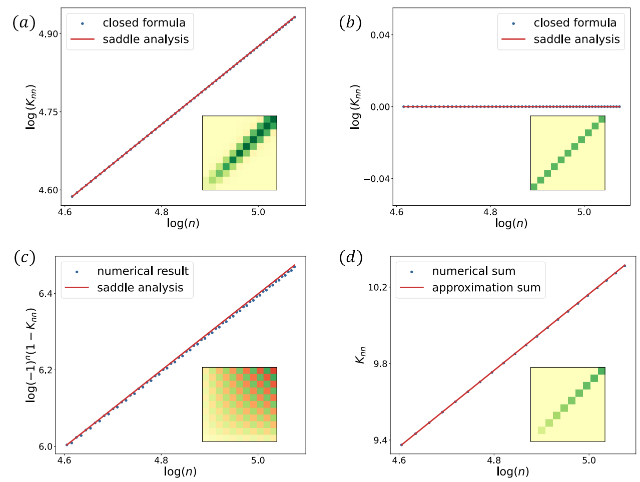

FIG. 2. We present the plot of the Krylov metric for (a) the SYK model with $h = 3/4$, (b) the SYK model with $h = 0$, (c) the Luttinger liquids with $\Delta = 1$, and (d) MBL systems with $\xi = 1$. In each sub-figure, we also show a matrix plot of K_{mn} as an inset, where yellow, red and green represent zero, negative and positive numbers, respectively. For Luttinger liquids, the matrix plot only contains K_{mn} with even indices so that they are real.

Accorcding to (3), its Taylor expansion in y_1 and y_2 should be matched with $\sum_{mn} D_m D_n K_{mn} y_1^m y_2^n$. The result can be computed in closed-form. We leave the complete expression in the supplementary material [72], where we confirmed that K_{mn} is dominated by the diagonal element

$$K_{nn} \propto \frac{\Gamma(h+n+2\Delta)\,{}_3F_2(-h,-h,-n;1,-h-n-2\Delta+1;1)}{\Gamma(h+2\Delta)\Gamma(n+2\Delta)}. \tag{10}$$

Here, ${}_3F_2$ represents the generalized hypergeometric function. When we expand the result in the limit of $n \to \infty$, we derive the following asymptotic behaviors (also see FIG. 2 (a-b)): (i) the diagonal elements satisfy: $K_{nn} \propto n^h = n^{\varkappa/(2\alpha)}$, notice this produces a constant K_{nn} in the dissipative limit $u/J \to 0$, where the quantum Lyapunov exponent vanishes, while the Krylov exponent is $\alpha = 2\pi/\beta$; (ii) for generic $0 < h < 1$, the off-diagonal elements scale as: $K_{n+m,n-m} \propto K_{nn}m^{-2h-1}$ for $n \gg m \gg 1$, i.e. they exhibit power-law decay along the orthogonal off-diagonal direction; (iii) in the limit of either the dissipative or maximally chaotic phase $h \to \{0, 1\}$, the Krylov metric K_{mn} approaches being exactly diagonal. These behaviors can also be explicitly derived through a saddle-point analysis [72].

Example 2: Luttinger Liquids.– We now turn to the investigation of free CFTs, as an extreme example of non-chaotic systems. We consider Luttinger liquids, which describes a large class of gapless quantum matters in 1+1D [59]. The Hamiltonian reads

$$H = \frac{u}{2\pi}\int dx\left[\frac{1}{K}(\nabla\hat{\phi}(x))^2 + K(\pi\hat{\Pi}(x))^2\right]. \tag{11}$$

where K is the Luttinger parameter and u is the sound velocity.

$\hat{\phi}(x)$ is a scalar field with conjugate momentum $\hat{\Pi}(y)$, which satisfies the canonical commutation relation $[\hat{\phi}(x), \hat{\Pi}(y)] = i\delta(x-y)$. We focus on the vertex operator $\hat{O} \sim: e^{-in_0\hat{\phi}(x)}:$, where : : denotes normal ordering. The two-point function is determined by the conformal symmetry $G(t) = (\cosh(\alpha t))^{-2\Delta}$ with scaling dimension $\Delta = Kn_0^2/4$. Since this two-point function takes the same form as in the SYK model, the Lanczos coefficients and the operator wavefunction are still given by (7). We then proceed to compute the OTOC. Taking $\hat{O}' \sim: e^{in_0\hat{\phi}(x)}:$, the result of OTOC reads:

$$F(t_1,t_2) = G(t_{12})\left(1-\left[\frac{\cosh(\alpha t_{12}) - i\sinh(2\alpha T_{12})}{\cosh(\alpha t_{12}) + i\sinh(2\alpha T_{12})}\right]^{2\Delta}\right). \tag{12}$$

The Krylov metric K_{mn} is computed using a strategy similar to that of Eq. (27). Since the conotribution from the first term in (12) is δ_{mn}, we only focus on the second term. Unfortunately, we are unable to compute its expansion in closed form. Instead, we represent it as a contour integral:

$$K_{mn} = \frac{D_m^{-1}D_n^{-1}}{(2\pi i)^2}\oint_C \frac{dy_1}{y_1^{m+1}}\oint_C \frac{dy_2}{y_2^{n+1}}\Big[\prod_i \cosh(\alpha t_i)^{2\Delta}\Big]F(t_1,t_2), \tag{13}$$

where the integrand should be viewed as functions of $y_{1,2}$. The integral contour C is along the unit circle, which encloses the origin counterclockwise. We can extract the asymptotic form of K_{mn} for $n, m \gg 1$ by evaluate the contour integral (13) using the saddle-point approximation. We find that:

$$K_{mn} \sim (-1)^{\frac{m+n}{2}}(mn)^{\Delta-1/2} \tag{14}$$

This result reveals two important observations: (i) The diagonal components K_{nn} exhibit alternating signs when n is changed, leading to a cancellation effect among different n values. (ii) The off-diagonal components K_{mn} are comparable to the diagonal components, see FIG. 2 (c). As a result, the summation in (3) experiences significant cancellation, distinguishing Luttinger liquids from the SYK model.

Example 3: MBL systems.– Finally, we consider cases that lie in between chaotic systems and non-interacting systems. A celebrated example is systems exhibiting many-body localization [60–66]. We examine the effective Hamiltonian [64–66]

$$H = \frac{1}{2}\sum_{i\neq j} J_{ij}\hat{\sigma}_z^i\hat{\sigma}_z^j + \sum_i h_i\hat{\sigma}_z^i + ... \tag{15}$$

This model is believed to capture the essential features of MBL systems. In particular, it commutes with an extensive number of mutually commuting operators σ_z^i, known as local integrals of motion (LIOM). ... denotes possible higher-order terms, which describes multi-body interactions between LIOMs. For simplicity, we neglect their contributions to correlation functions. We model random couplings J_{ij} and magnetic field h_i as independent Gaussian varibles with zero means and

$$\overline{J_{ij}^2} = J^2 e^{-\frac{|i-j|}{\xi}}, \qquad \overline{h_i^2} = h^2. \tag{16}$$

Here, ξ is known as the localization length, which characterize the interaction range between LIOMs. We expect the physical results do not reply on details of the distribution function.

We choose $\hat{O} = \hat{\sigma}_x^0$ that flips LIOMs. In localized systems, the violation of thermalization renders finite temperature ensembles meaningless. Therefore, all calculations are performed at infinite temperature. The Lanzcos coeffcients are then fixed by the auto-correlation function, which reads $G(t) = \overline{\prod_{j\neq 0}\cos(2J_{0j}t)\cos(2h_0 t)} = e^{-\frac{\gamma^2 t^2}{2}}$. Here, we averaged over the random couplings and introduced $\gamma^2 = 4(J^2\sum_{j\neq 0} e^{-|j|/\xi} + h^2)$. The result shows that the auto-correlation function decays as a Gaussian function, of which the Krylov basis wavefunction and the Lanzcos coefficients are known as [48]

$$b_n = \gamma\sqrt{n} \qquad \varphi_n(t) = \frac{\gamma^n t^n}{\sqrt{n!}}e^{-\frac{\gamma^2 t^2}{2}}, \tag{17}$$

and the Krlov complexity grows quadratically $\mathcal{K}(t) = \gamma^2 t^2$. We proceed to investigate the behavior of Krylov metric. Choosing $\hat{O} = \hat{\sigma}_x^m$ and performing an average over site m, we find

$$\overline{F(t_1,t_2)} = e^{-\frac{\gamma^2 t_{12}^2}{2}} - N^{-1}e^{-2\gamma^2 T_{12}^2} - \sum_{m\neq 0} N^{-1}e^{-8J^2 e^{-\frac{|m|}{\xi}} t_1 t_2 - \frac{\gamma^2 t_{12}^2}{2}}. \tag{18}$$

Here, N denotes total number of sites. Using (3), we find the Krylov metric takes a purely diagonal form, see Figure (2):

$$K_{mn} = K_{nn}\delta_{mn}, \quad K_{nn} \approx \frac{2\xi}{N}\ln\left(\frac{8J^2 n}{\gamma^2}\right). \tag{19}$$

This $\ln n$ behavior is a signature of logarithmic lightcones in the MBL system [73–78]. Although the Krylov complexity grows quadratically, the operator size in MBL systems only increases as $\ln t$. The scaling analysis then suggests $K_{nn} \sim \log n$, supported in FIG. 2 (d). This example demonstrates the usefulness of the Krylov metric beyond identifying fast scramblers, indicating its broad application in characterizing quantum dynamics.

Size-resolved Metric– Given the general interpretation of the OTOC in terms of the operator size growth, more refined information of the Krylov metric can be revealed by resolving it using the operator size distribution. In lattice models where operator sizes can be explicitly defined, we can perform the following decomposition:

$$K_{mn} = \sum_\ell K_{mn}(\ell), \quad K_{mn}(\ell) = \ell\langle O_m|\hat{P}(\ell)|O_n\rangle \tag{20}$$

where $\hat{P}(\ell)$ is the projector into the operator Hilbert space sector of fixed size ℓ. The decomposition $K_{mn}(\ell)$ can be retrieved by first computing and then expanding the operator-size generating functions. The details of these computations can be found in the supplementary material [72]. For the SYK models, the scramblon calculations [79, 80] predict that the resolved metric $K_{mn}(\ell)$ takes the factorized form $K_{mn}(\ell) = \ell J_m(\ell)J_n(\ell)$. The factorization indicates the following structure of the operator wave-function$|O_n\rangle = \sum_\ell J_n(\ell)\;|\chi_\ell\rangle$. i.e.

the projection onto operator size ℓ is identical for all O_n. We expect this as a result of the permutation symmetric Hamiltonians. Upon scaling the operator size as: $\ell^{1/\varkappa} \propto \lambda n$, we obtain the asymptotic behavior

$$J_n(\ell) \sim n^{-\varkappa/2}\left[e^{\sqrt{\lambda(\lambda-4)}}\left(\lambda-2-\sqrt{\lambda(\lambda-4)}\right)\right]^{-n} \tag{21}$$

This implies that O_n has typical operator size $\ell \sim n^{\varkappa}$. The operator weight shows a phase transition between oscillatory behavior for $\lambda < 4$ to exponential decay for $\lambda > 4$. For the MBL systems, the resolved Krylov metric $K_{mn}(\ell) = K_{nn}(\ell)\delta_{mn}$ remains exactly diagonal. This indicates that the projections from distinct $O_{m\neq n}$ onto any fixed operator length ℓ are orthogonal. Upon scaling the operator size as: $\ell \propto \lambda \ln n$, we obtain the asymptotic behavior

$$K_{nn}(\ell) \sim \lambda\, e^{-\frac{(\lambda-\xi)^2}{\xi}\ln n} \tag{22}$$

This implies a Gaussian distribution in the operator size ℓ with comparable mean and variance: $\langle\ell\rangle \sim \delta^2 \sim \xi \ln n$.

Discussions.– In this work, we introduced the Krylov metric K_{mn} to bridge the gap between the growth of Krylov complexity and quantum many-body chaos. Physically, the Krylov metric measures the size growth in the Krylov space, which captures intrinsic properties of the Krylov basis. With a combination of the Krylov metric and Lanczos coefficients, we are able to provide criterion for fast scramblers, which require power-law growing diagonal components with negligible off-diagonal components for K_{mn}, in addition to exponential growing Krylov complexity. These criteria are supported by analytical studies in the SYK model, Luttinger liquids, and MBL systems.

We conclude with some proposals for future investigations. Firstly, while our criterion in terms of the Krylov metric provide sufficient conditions for fast scramblers, it is important to understand to what extent are they also necessary. Secondly, having decomposed the lyapunov exponent $\varkappa = 2\alpha h$ into factors from the Krylov complexity α and the Krylov metric h, we need to understand the physical roles each factor plays. For example, how do they reflect different aspects of the underlying mechanism for quantum many-body chaos? Lastly, equipped with the perspective of the Krylov metric, we can explore systems exhibiting novel behaviors beyond the ones identified in this work. This will possibly shed lights on new aspects of quantum chaos.

Acknowledgment. We thank Zhao-Yi Zeng and Ren Zhang for helpful discussions. This project is supported by the NSFC under grant No. 12175238, 12374477, 12247103.

* wanghuajia@ucas.ac.cn
† PengfeiZhang.physics@gmail.com

[1] P. Hayden and J. Preskill, Black holes as mirrors: Quantum information in random subsystems, JHEP **09**, 120, arXiv:0708.4025 [hep-th].
[2] Y. Sekino and L. Susskind, Fast Scramblers, JHEP **10**, 065, arXiv:0808.2096 [hep-th].
[3] T. Dray and G. 't Hooft, The gravitational shock wave of a massless particle, Nuclear Physics B **253**, 173 (1985).
[4] G. 't Hooft, The black hole interpretation of string theory, Nuclear Physics B **335**, 138 (1990).
[5] Y. Kiem, H. L. Verlinde, and E. P. Verlinde, Black hole horizons and complementarity, Phys. Rev. D **52**, 7053 (1995), arXiv:hep-th/9502074.
[6] G. 't Hooft, The Scattering matrix approach for the quantum black hole: An Overview, Int. J. Mod. Phys. A **11**, 4623 (1996), arXiv:gr-qc/9607022.
[7] A. I. Larkin and Y. N. Ovchinnikov, Quasiclassical Method in the Theory of Superconductivity, Soviet Journal of Experimental and Theoretical Physics **28**, 1200 (1969).
[8] S. H. Shenker and D. Stanford, Black holes and the butterfly effect, JHEP **03**, 067, arXiv:1306.0622 [hep-th].
[9] S. H. Shenker and D. Stanford, Stringy effects in scrambling, JHEP **05**, 132, arXiv:1412.6087 [hep-th].
[10] A. Kitaev, talk given at fundamental physics prize symposium (2014).
[11] D. A. Roberts, D. Stanford, and L. Susskind, Localized shocks, JHEP **03**, 051, arXiv:1409.8180 [hep-th].
[12] D. A. Roberts, D. Stanford, and A. Streicher, Operator growth in the SYK model, JHEP **06**, 122, arXiv:1802.02633 [hep-th].
[13] X.-L. Qi and A. Streicher, Quantum Epidemiology: Operator Growth, Thermal Effects, and SYK, JHEP **08**, 012, arXiv:1810.11958 [hep-th].
[14] J. Maldacena, S. H. Shenker, and D. Stanford, A bound on chaos, JHEP **08**, 106, arXiv:1503.01409 [hep-th].
[15] A. Kitaev, A simple model of quantum holography (part 1), Kavli Institute for Theoretical Physics Program: Entanglement in Strongly-Correlated Quantum Matter (Apr 6 - Jul 2, 2015). (2015).
[16] S. Sachdev and J. Ye, Gapless spin-fluid ground state in a random quantum heisenberg magnet, Phys. Rev. Lett. **70**, 3339 (1993).
[17] J. Maldacena and D. Stanford, Remarks on the Sachdev-Ye-Kitaev model, Phys. Rev. D **94**, 106002 (2016), arXiv:1604.07818 [hep-th].
[18] A. Kitaev and S. J. Suh, The soft mode in the Sachdev-Ye-Kitaev model and its gravity dual, JHEP **05**, 183, arXiv:1711.08467 [hep-th].
[19] D. Chowdhury, A. Georges, O. Parcollet, and S. Sachdev, Sachdev-Ye-Kitaev models and beyond: Window into non-Fermi liquids, Rev. Mod. Phys. **94**, 035004 (2022), arXiv:2109.05037 [cond-mat.str-el].
[20] S. Xu and B. Swingle, Scrambling Dynamics and Out-of-Time-Ordered Correlators in Quantum Many-Body Systems, PRX Quantum **5**, 010201 (2024), arXiv:2202.07060 [quant-ph].
[21] X. Chen and T. Zhou, Quantum chaos dynamics in long-range power law interaction systems, Phys. Rev. B **100**, 064305 (2019), arXiv:1808.09812 [cond-mat.stat-mech].
[22] T. Zhou and X. Chen, Operator dynamics in a Brownian quantum circuit, Phys. Rev. E **99**, 052212 (2019), arXiv:1805.09307 [cond-mat.str-el].
[23] J. Maldacena, D. Stanford, and Z. Yang, Diving into traversable wormholes, Fortsch. Phys. **65**, 1700034 (2017), arXiv:1704.05333 [hep-th].
[24] D. A. Roberts and B. Yoshida, Chaos and complexity by design, JHEP **04**, 121, arXiv:1610.04903 [quant-ph].
[25] R. Jefferson and R. C. Myers, Circuit complexity in quantum field theory, JHEP **10**, 107, arXiv:1707.08570 [hep-th].
[26] R.-Q. Yang, Complexity for quantum field theory states and ap-

plications to thermofield double states, Phys. Rev. D **97**, 066004 (2018), arXiv:1709.00921 [hep-th].
[27] S. Chapman, M. P. Heller, H. Marrochio, and F. Pastawski, Toward a Definition of Complexity for Quantum Field Theory States, Phys. Rev. Lett. **120**, 121602 (2018), arXiv:1707.08582 [hep-th].
[28] R. Khan, C. Krishnan, and S. Sharma, Circuit Complexity in Fermionic Field Theory, Phys. Rev. D **98**, 126001 (2018), arXiv:1801.07620 [hep-th].
[29] R.-Q. Yang, Y.-S. An, C. Niu, C.-Y. Zhang, and K.-Y. Kim, Principles and symmetries of complexity in quantum field theory, Eur. Phys. J. C **79**, 109 (2019), arXiv:1803.01797 [hep-th].
[30] A. Lucas, Operator size at finite temperature and Planckian bounds on quantum dynamics, Phys. Rev. Lett. **122**, 216601 (2019), arXiv:1809.07769 [cond-mat.str-el].
[31] V. Balasubramanian, M. Decross, A. Kar, and O. Parrikar, Quantum Complexity of Time Evolution with Chaotic Hamiltonians, JHEP **01**, 134, arXiv:1905.05765 [hep-th].
[32] V. Balasubramanian, M. DeCross, A. Kar, Y. C. Li, and O. Parrikar, Complexity growth in integrable and chaotic models, JHEP **07**, 011, arXiv:2101.02209 [hep-th].
[33] D. E. Parker, X. Cao, A. Avdoshkin, T. Scaffidi, and E. Altman, A Universal Operator Growth Hypothesis, Phys. Rev. X **9**, 041017 (2019), arXiv:1812.08657 [cond-mat.stat-mech].
[34] A. Avdoshkin, A. Dymarsky, and M. Smolkin, Krylov complexity in quantum field theory, and beyond, arXiv e-prints , arXiv:2212.14429 (2022), arXiv:2212.14429 [hep-th].
[35] V. Balasubramanian, P. Caputa, J. M. Magan, and Q. Wu, Quantum chaos and the complexity of spread of states, Phys. Rev. D **106**, 046007 (2022), arXiv:2202.06957 [hep-th].
[36] C. Liu, H. Tang, and H. Zhai, Krylov complexity in open quantum systems, Physical Review Research **5**, 033085 (2023), arXiv:2207.13603 [cond-mat.str-el].
[37] J. L. F. Barbón, E. Rabinovici, R. Shir, and R. Sinha, On The Evolution Of Operator Complexity Beyond Scrambling, JHEP **10**, 264, arXiv:1907.05393 [hep-th].
[38] A. Dymarsky and A. Gorsky, Quantum chaos as delocalization in Krylov space, Phys. Rev. B **102**, 085137 (2020), arXiv:1912.12227 [cond-mat.stat-mech].
[39] J. L. F. Barbón, J. Martín-García, and M. Sasieta, Momentum/Complexity Duality and the Black Hole Interior, JHEP **07**, 169, arXiv:1912.05996 [hep-th].
[40] J. M. Magán and J. Simón, On operator growth and emergent Poincaré symmetries, JHEP **05**, 071, arXiv:2002.03865 [hep-th].
[41] S.-K. Jian, B. Swingle, and Z.-Y. Xian, Complexity growth of operators in the SYK model and in JT gravity, JHEP **03**, 014, arXiv:2008.12274 [hep-th].
[42] E. Rabinovici, A. Sánchez-Garrido, R. Shir, and J. Sonner, Operator complexity: a journey to the edge of Krylov space, JHEP **06**, 062, arXiv:2009.01862 [hep-th].
[43] C.-F. Chen and A. Lucas, Operator Growth Bounds from Graph Theory, Commun. Math. Phys. **385**, 1273 (2021), arXiv:1905.03682 [math-ph].
[44] J. D. Noh, Operator growth in the transverse-field Ising spin chain with integrability-breaking longitudinal field, Phys. Rev. E **104**, 034112 (2021), arXiv:2107.08287 [quant-ph].
[45] P. Caputa and S. Datta, Operator growth in 2d CFT, JHEP **12**, 188, [Erratum: JHEP 09, 113 (2022)], arXiv:2110.10519 [hep-th].
[46] D. Patramanis, Probing the entanglement of operator growth, PTEP **2022**, 063A01 (2022), arXiv:2111.03424 [hep-th].
[47] B. Bhattacharjee, X. Cao, P. Nandy, and T. Pathak, Krylov complexity in saddle-dominated scrambling, JHEP **05**, 174, arXiv:2203.03534 [quant-ph].
[48] P. Caputa, J. M. Magan, and D. Patramanis, Geometry of Krylov complexity, Phys. Rev. Res. **4**, 013041 (2022), arXiv:2109.03824 [hep-th].
[49] A. Dymarsky and M. Smolkin, Krylov complexity in conformal field theory, Phys. Rev. D **104**, L081702 (2021), arXiv:2104.09514 [hep-th].
[50] A. Avdoshkin and A. Dymarsky, Euclidean operator growth and quantum chaos, Phys. Rev. Res. **2**, 043234 (2020), arXiv:1911.09672 [cond-mat.stat-mech].
[51] E. Rabinovici, A. Sánchez-Garrido, R. Shir, and J. Sonner, A bulk manifestation of Krylov complexity, JHEP **08**, 213, arXiv:2305.04355 [hep-th].
[52] C. Liu, H. Tang, and H. Zhai, Krylov complexity in open quantum systems, Phys. Rev. Res. **5**, 033085 (2023), arXiv:2207.13603 [cond-mat.str-el].
[53] A. Bhattacharya, P. Nandy, P. P. Nath, and H. Sahu, Operator growth and Krylov construction in dissipative open quantum systems, JHEP **12**, 081, arXiv:2207.05347 [quant-ph].
[54] B. Bhattacharjee, X. Cao, P. Nandy, and T. Pathak, Operator growth in open quantum systems: lessons from the dissipative SYK, JHEP **03**, 054, arXiv:2212.06180 [quant-ph].
[55] B. Bhattacharjee, P. Nandy, and T. Pathak, Operator dynamics in Lindbladian SYK: a Krylov complexity perspective, JHEP **01**, 094, arXiv:2311.00753 [quant-ph].
[56] C. Lv, R. Zhang, and Q. Zhou, Building Krylov complexity from circuit complexity, arXiv e-prints , arXiv:2303.07343 (2023), arXiv:2303.07343 [quant-ph].
[57] H. Tang, Operator Krylov complexity in random matrix theory, arXiv e-prints , arXiv:2312.17416 (2023), arXiv:2312.17416 [hep-th].
[58] R. Zhang and H. Zhai, Universal Hypothesis of Autocorrelation Function from Krylov Complexity, arXiv e-prints , arXiv:2305.02356 (2023), arXiv:2305.02356 [cond-mat.stat-mech].
[59] T. Giamarchi, *Quantum Physics in One Dimension* (Oxford University Press, 2003).
[60] D. A. Abanin, E. Altman, I. Bloch, and M. Serbyn, Colloquium: Many-body localization, thermalization, and entanglement, Rev. Mod. Phys. **91**, 021001 (2019).
[61] F. Alet and N. Laflorencie, Many-body localization: An introduction and selected topics, Comptes Rendus Physique **19**, 498 (2018), arXiv:1711.03145 [cond-mat.str-el].
[62] E. Altman and R. Vosk, Universal Dynamics and Renormalization in Many-Body-Localized Systems, Annual Review of Condensed Matter Physics **6**, 383 (2015), arXiv:1408.2834 [cond-mat.dis-nn].
[63] R. Nandkishore and D. A. Huse, Many-Body Localization and Thermalization in Quantum Statistical Mechanics, Annual Review of Condensed Matter Physics **6**, 15 (2015), arXiv:1404.0686 [cond-mat.stat-mech].
[64] M. Serbyn, Z. Papić, and D. A. Abanin, Local conservation laws and the structure of the many-body localized states, Phys. Rev. Lett. **111**, 127201 (2013).
[65] D. A. Huse, R. Nandkishore, and V. Oganesyan, Phenomenology of fully many-body-localized systems, Phys. Rev. B **90**, 174202 (2014).
[66] R. Vosk and E. Altman, Many-body localization in one dimension as a dynamical renormalization group fixed point, Phys. Rev. Lett. **110**, 067204 (2013).
[67] Notice that our convention for the Liouvillian superoperator differs from that in [33] by a factor of i.
[68] C. Lanczos, An iteration method for the solution of the eigenvalue problem of linear differential and integral operators, J.

Res. Natl. Bur. Stand. B **45**, 255 (1950).
[69] Z. Liu and P. Zhang, Signature of Scramblon Effective Field Theory in Random Spin Models, Phys. Rev. Lett. **132**, 060201 (2024), arXiv:2306.05678 [quant-ph].
[70] Y. Chen, H. Zhai, and P. Zhang, Tunable Quantum Chaos in the Sachdev-Ye-Kitaev Model Coupled to a Thermal Bath, JHEP **07**, 150, arXiv:1705.09818 [hep-th].
[71] P. Zhang and Z. Yu, Dynamical Transition of Operator Size Growth in Quantum Systems Embedded in an Environment, Phys. Rev. Lett. **130**, 250401 (2023).
[72] See supplementary material for: (1). Detailed derivations of the asymptotic behaviors of the Krylov metric; (2). Detailed computations of the operator-size distribution of the Krylov metric.
[73] Y. Huang, Y.-L. Zhang, and X. Chen, Out-of-time-ordered correlators in many-body localized systems, Annalen Phys. **529**, 1600318 (2017), arXiv:1608.01091 [cond-mat.dis-nn].
[74] R. Fan, P. Zhang, H. Shen, and H. Zhai, Out-of-Time-Order Correlation for Many-Body Localization, Sci. Bull. **62**, 707 (2017), arXiv:1608.01914 [cond-mat.quant-gas].
[75] B. Swingle and D. Chowdhury, Slow scrambling in disordered quantum systems, Phys. Rev. B **95**, 060201 (2017), arXiv:1608.03280 [cond-mat.str-el].
[76] R.-Q. He and Z.-Y. Lu, Characterizing many-body localization by out-of-time-ordered correlation, Phys. Rev. B **95**, 054201 (2017), arXiv:1608.03586 [cond-mat.dis-nn].
[77] Y. Chen, Universal Logarithmic Scrambling in Many Body Localization, arXiv e-prints , arXiv:1608.02765 (2016), arXiv:1608.02765 [cond-mat.dis-nn].
[78] X. Chen, T. Zhou, D. A. Huse, and E. Fradkin, Out-of-time-order correlations in many-body localized and thermal phases, Annalen der Physik **529**, 1600332 (2017), arXiv:1610.00220 [cond-mat.str-el].
[79] Y. Gu, A. Kitaev, and P. Zhang, A two-way approach to out-of-time-order correlators, JHEP **03**, 133, arXiv:2111.12007 [hep-th].
[80] P. Zhang and Y. Gu, Operator size distribution in large N quantum mechanics of Majorana fermions, JHEP **10**, 018, arXiv:2212.04358 [cond-mat.str-el].

Supplemental Material: Dissecting Quantum Many-body Chaos in the Krylov Space

In this suppelmentary material, we provide additional details for the calculations done in the main text.

ASYMPTOTIC BEHAVIORS OF K_{mn}

The connected part of the OTOCs $F(t_1,t_2)$ at late times are controlled by the asymptotic behaviors of the corresponding Krylov metric K_{mn}, which are related by:

$$F(t_1,t_2) = \sum_{m,n} K_{mn}\ \varphi_m(t_1)\varphi_n(t_2)^* \tag{23}$$

The operator wave-functions $\varphi_n(t)$ depend on the auto-correlation function. In cases where they admit simple n-dependences, it is possible to perform the conversion explicitly. More explicitly, for $\varphi_n(t)$ of the general form:

$$\varphi_n(t) = D(n)h(t)y(t)^n \tag{24}$$

We can extract the Krylov by expanding $F(t_1,t_2)$ in powers of $y(t_1)$ and $y(t_2)$, which in turn can be written as double contour integrals:

$$K_{mn} = D(n)^{-1}D(m)^{-1}\oint\frac{dy_1}{y_1^{n+1}}\oint\frac{dy_2}{y_2^{m+1}}h(t_1)^{-1}h(t_2)^{-1}F(t_1,t_2) \tag{25}$$

where the integrand can be viewed implicitly as functions of the $y_{1,2} = y(t_{1,2})$. For the interest of large order asymptotics $m,n \gg 1$, we can use m,n as large parameters to perform saddle-point approximations for evaluating these contour integrals. In this section, we derive the asymptotic behaviors of K_{mn} for the three classes of models considered in the main text.

Example 1: the SYK models

We begin with the example of the SYK models. Quoting the expressions for $F(t_1,t_2)$ and $\varphi_n(t)$ in the main text gives:

$$\begin{aligned} F(t_1,t_2) &= G(t_1+t_2)\,H(t_1-t_2)\,,\quad G(t)=e^{h\alpha t},\quad H(t)=\cosh(\alpha t)^{-2\Delta-h} \\ \varphi(t) &= \frac{\tanh(\alpha t)^n}{\cosh(\alpha t)^{2\Delta}}D(n),\quad D(n)=\sqrt{\frac{\Gamma(2\Delta+n)}{\Gamma(n+1)\Gamma(2\Delta)}} \end{aligned} \tag{26}$$

In this case, we can obtain an exact analytic expression for K_{mn} by identifying $y_{1,2} = \tanh(\alpha t_{1,2})$ and writing:

$$\cosh(\alpha t_1)^{2\Delta}\cosh(\alpha t_2)^{2\Delta}F(t_1,t_2) \propto \frac{(1+y_1)^h(1+y_2)^h}{(1-y_1y_2)^{h+2\Delta}} = \sum_{mn} D_mD_nK_{mn}y_1^my_2^n \tag{27}$$

Here we fixed the normalization condition $K_{00}=1$. The Krylove metric K_{mn} can be obtained by expanding each factor in the RHS of (27) in terms of $y_{1,2}$:

$$(1+y)^h = \sum_{n=0}^{\infty}\frac{\Gamma(h+1)}{\Gamma(n+1)\Gamma(h+1-n)}y^n,\qquad \frac{1}{(1-y_1y_2)^D} = \sum_{n=0}^{\infty}\frac{\Gamma(n+D)}{\Gamma(n+1)\Gamma(D)}y_1^ny_2^n. \tag{28}$$

Since K_{mn} is symmetric in m and n, we assume $m \geq n$. This gives:

$$\begin{aligned} K_{mn} &= \sqrt{\frac{\Gamma(n+1)\Gamma(2\Delta)}{\Gamma(2\Delta+n)}}\sqrt{\frac{\Gamma(m+1)\Gamma(2\Delta)}{\Gamma(2\Delta+m)}}\sum_{k=0}^{n}\frac{\Gamma(h+1)}{\Gamma(n-k+1)\Gamma(h+1-n+k)} \\ &\quad\times\frac{\Gamma(h+1)}{\Gamma(m-k+1)\Gamma(h+1-m+k)}\frac{\Gamma(h+k+2\Delta)}{\Gamma(k+1)\Gamma(h+2\Delta)} \\ &= \sqrt{\frac{\Gamma(2\Delta)}{\Gamma(n+1)\Gamma(2\Delta+n)}}\sqrt{\frac{\Gamma(2\Delta)}{\Gamma(m+1)\Gamma(2\Delta+m)}}\Gamma(h+1)^2 \\ &\quad\times\frac{{}_3F_2(-m,-n,h+2\Delta;h-m+1,h-n+1;1)}{\Gamma(h-m+1)\Gamma(h-n+1)} \end{aligned} \tag{29}$$

Here ${}_3F_2$ is the generalized hypergeometric function. In particular, for $m = n$, the result reduces to

$$K_{nn} = \frac{\Gamma(2\Delta)\Gamma(h+n+2\Delta)\,{}_3F_2(-h,-h,-n;1,-h-n-2\Delta+1;1)}{\Gamma(h+2\Delta)\Gamma(n+2\Delta)}. \tag{30}$$

Given the exact result (30) for K_{mn}, we are more interested in its asymptotic behaviors. This can be more readily obtained via the contour integrals representation of K_{mn} about $y_1 = y_2 = 0$ and performing the suggested saddle-point analysis. We proceed by parameterizing both by their the phase variables $y_{1,2} = e^{\theta_{1,2}}$. The contour integral can thus be written as:

$$K_{mn} = D(m)^{-1}D(n)^{-1}\int d\theta_1 d\theta_2\; e^{-S(\theta_1,\theta_2)} \tag{31}$$

where the effective action S is given by:

$$\begin{aligned} S(\theta_1,\theta_2) &= m\theta_1 + n\theta_2 + (2\Delta+h)\ln\left(1-e^{\theta_1+\theta_2}\right) \\ &- h\ln\left(1+e^{\theta_1}\right) - h\ln\left(1+e^{\theta_2}\right) \end{aligned} \tag{32}$$

Treating $m, n \gg 1$ as the large parameters, the saddle-point equations becomes:

$$m = \frac{he^{\theta_1}}{1+e^{\theta_1}} + \frac{(2\Delta+h)e^{\theta_1+\theta_2}}{1-e^{\theta_1+\theta_2}}, \quad n = \frac{he^{\theta_1}}{1+e^{\theta_2}} + \frac{(2\Delta+h)e^{\theta_1+\theta_2}}{1-e^{\theta_1+\theta_2}} \tag{33}$$

The solution takes the form:

$$\begin{aligned} e^{\theta_1^*} &= -\frac{h^2+2(n-m)(m+\Delta) \pm \sqrt{h^4+4(n-m)^2\Delta^2+4h^2\left(mn+(m+n)\Delta\right)}}{2(h+n-m)(m+2\Delta)} \\ e^{\theta_2^*} &= -\frac{h^2+2(m-n)(n+\Delta) \pm \sqrt{h^4+4(n-m)^2\Delta^2+4h^2\left(mn+(m+n)\Delta\right)}}{2(h+m-n)(n+2\Delta)} \end{aligned}$$

We analyze the properties of the saddle in different limits of $M, N \gg 1$.

- $\boldsymbol{n = L(1+\lambda),\ m = L(1-\lambda),\ \ 0 < \lambda < 1}$**:**

  In this limit, the entry is away from the diagonal by the same order as m, n, and the parameter λ denotes the orthogonal distance to the diagonal. The dominant saddle point admits an expansion in large L:

$$\begin{aligned} \theta_1^* &= i\pi - \frac{2\Delta\lambda + h(1-\lambda) - \sqrt{h^2(1-\lambda^2)+4\Delta\lambda^2}}{2L\lambda(1-\lambda)} + \ldots \\ \theta_2^* &= i\pi - \frac{2\Delta\lambda - h(1+\lambda) + \sqrt{h^2(1-\lambda^2)+4\Delta\lambda^2}}{2L\lambda(1+\lambda)} + \ldots \end{aligned} \tag{34}$$

  Plugging this back to the effective action gives, we can estimate the large order behavior of the Krylov kernel:

$$K_{mn} \sim L^{-h+1}\lambda^{-2h} \times (\text{fluctuation}) \tag{35}$$

  where we have kept only the leading order dependence on finite but small λ, The fluctuation part comes from the integral about the saddle point. Expanding near the (θ_1^*, θ_2^*), it can be checked that the effective action takes the form:

$$S(\theta_1,\theta_2) = S^* + A_+L^2\delta\theta_+^2 + A_-L^2\lambda^2\delta\theta_-^2 + \sum_{p+q\geq 3} S_{pq}\,\delta\theta_+^p\,\delta\theta_-^q, \quad S_{pq} \sim L^{p+q}\lambda^q$$

  where $A_\pm$ are $O(1)$ constants and $\delta\theta_\pm$ are eigen-modes of the Hessian matrix. At the leading order in $L \gg 1$ they simply correspond to:

$$\delta\theta_+ = \delta\theta_1 + \delta\theta_2, \quad \delta\theta_+ = \delta\theta_1 - \delta\theta_2, \quad \delta\theta_{1,2} = \theta_{1,2} - \theta_{1,2}^* \tag{36}$$

  We can therefore extract an additional factor of $L^{-2}\lambda^{-1}$ from the fluctuation by rescaling the integration variables $\delta\theta_+ = \delta\tilde{\theta}_+/L, \delta\theta_- = \delta\tilde{\theta}_-/(L\lambda)$, and leaving the remaining integral as an order 1 factor:

$$\int_{-\pi}^{\pi} d\delta\theta_+ \int_{-\pi}^{\pi} d\delta\theta_-\; e^{-\sum_{p,q} S_{pq}\,\delta\theta_+^p\delta\theta_-^q} = \frac{1}{L^2\lambda}\left(\int_{-\infty}^{\infty} d\delta\tilde{\theta}_+ \int_{-\infty}^{\infty} d\delta\tilde{\theta}_-\; e^{-\sum_{p,q}\tilde{S}_{pq}\,\delta\tilde{\theta}_+^p\delta\tilde{\theta}_-^q}\right)$$

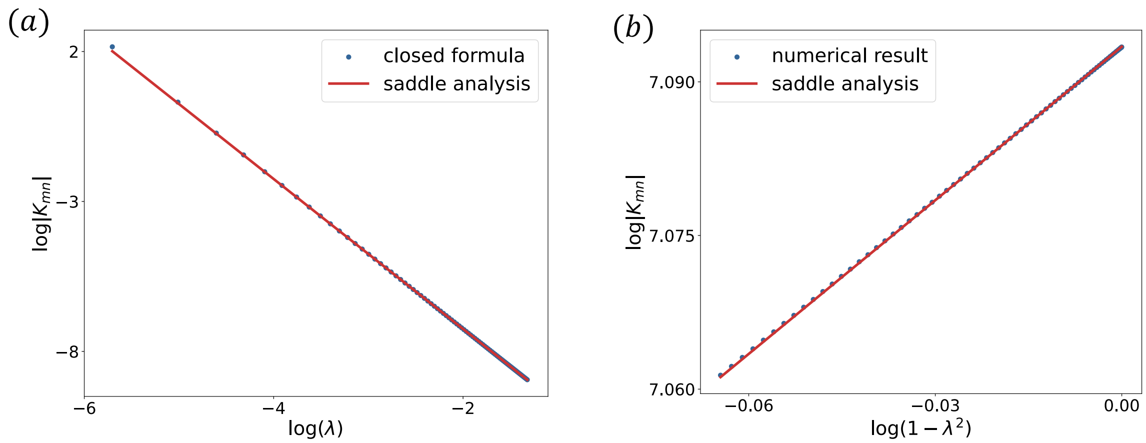

FIG. 3. We present the asymptotic behaviors of the orthogonal off-diagonal Krylov metric K_{mn} with $m = L(1-\lambda), n = L(1+\lambda)$ for: (a) the SYK model with $h = 3/4$, (b) the Luttinger liquids with $\Delta = 1$. In both cases, we have chosen $L = 300$.

where we now have $\tilde{S}_{pq} \sim \mathcal{O}(1)$ and the integration range of $\delta\tilde{\theta}_\pm$ has been set to $\pm\infty$ after the rescaling. We remark that this is slightly different from the usual scenario in performing the saddle-point analysis, in the sense that the fluctuations are not weakly coupled as Gaussians, yet whose contribution one can extract as a scaling factor comparable to S^*. Combining these we arrive at the estimates:

$$K_{mn} \sim L^{-h-1}\lambda^{-2h-1} \tag{37}$$

- $\boldsymbol{n = m = L}$**:**

  They correspond to matrix elements are lie exactly along the diagonal. The dominant saddle point now admits the expansion in large L:

$$\theta_1^* = \theta_2^* = -\frac{h+2\Delta}{2L} + \ldots \tag{38}$$

  Similar to before, this saddle-point evaluates to the following estimate:

$$K_{nn} \sim n^{h+1} \times (\text{fluctuation}) \tag{39}$$

  In this case, the fluctation analysis proceeds slightly differently. The expansion of the effective action now takes the form:

$$S(y_1, y_2) = S^* + \sum_{p,q} S_{pq}\delta\theta_+^p\delta\theta_-^q, \quad S_{pq} \sim L^p \tag{40}$$

  We see that in contrary to the previous case, the expansion coefficients scale with only one of the modes, i.e. $\delta\theta_+$. By the same logic as before, we can rescale $d\theta_+ = d\tilde{\theta}_+/L$, and after doing this we should extract an additional factor of L^{-1} from the fluctuation factor. As a result the diagonal Krylov kernel now exhibits the expected scaling behavior:

$$K_{nn} \sim n^h \tag{41}$$

Combining both limits, we summarize the asymptotic behaviors of K_{mn} as follows. The diagonal elements are given by:

$$K_{nn} \sim n^h \tag{42}$$

while the off-diagonal elements satisfy:

$$K_{mn} \sim K_{LL}|m-n|^{-2h-1}, \quad L = \frac{m+n}{2} \tag{43}$$

We also verify this off-diagonal result by doing numerical calculation directly, see FIG. 3 (a). In other words, the off-diagonal elements decay along the orthogonal off-diagonal direction as a power law with power $(-2h-1)$. This is sufficient for the dominance of the diagonal contribution for general h. In addition, it is also observed that the relative decay becomes singular for the immediate off-diagonal matrix elements as $h \to \{0, 1\}$:

$$\frac{K_{n,n+1}}{K_{nn}} \sim h(1-h), \quad \frac{K_{n,m}}{K_{n,m-1}} \sim O(1), \text{ for } (m-n) \geq 2 \tag{44}$$

Therefore, in the either the dissipative limit $h \to 0$ or the maximally chaotic limit $h \to 1$, the Krylov metric approaches being exactly diagonal. Capturing such phenomena however is beyond the scope of saddle-point approximations.

Example 2: Luttinger liquids

We begin the example of luttinger liquids by writing down the Hamiltonian as:

$$\begin{aligned} H &= \frac{u}{2\pi} \int dx \left[\frac{1}{K} (\nabla\phi(x))^2 + K (\pi\Pi(x))^2 \right] \\ &= \frac{u}{2\pi} \int dx \left[\frac{1}{K} (\nabla\phi(x))^2 + K (\nabla\theta(x))^2 \right] \end{aligned} \tag{45}$$

where $\nabla\theta(x)/\pi = \Pi(x)$ is the canonically conjugate momentum of $\phi(x)$, and the commutation relation can be written as:

$$\left[\phi(x), \frac{1}{\pi}\nabla\theta(x') \right] = i\delta(x - x') \tag{46}$$

One can then derive the following finite temperature correlation functions between general vertex operators [59]

$$\begin{aligned} I &= \left\langle \prod_j e^{iA_j\phi(r_j)} \right\rangle_\beta = e^{\frac{1}{2}\sum_{i<j}[(A_iA_jK)F(r_i-r_j)]} \\ F(r) &= \frac{1}{2}\log\left[\sinh^2\left(\frac{\pi x}{\beta u}\right) + \sin^2\left(\frac{\pi\tau}{\beta}\right) \right] \end{aligned} \tag{47}$$

Consider the vertex operator of scaling dimension $\Delta = Kn^2/4$:

$$V_n(x,t) =: \exp(in\phi(x,t)) : \tag{48}$$

Let us compute the thermally regulated OTOC of this operator:

$$C(t_1, t_2) = \langle V_{-n}(t_1 - i3\beta/4)V_n(-i\beta/2)V_n(t_2 - i\beta/4)V_{-n}(0)\rangle_\beta \tag{49}$$

Applying the general formula (47) to this computation then corresponds to setting the following non-zero parameters:

$$A_1 = -n, \quad A_2 = n, \quad A_3 = n, \quad A_4 = -n \tag{50}$$

and the corresponding coordinates are only separated in the time direction:

$$r_1 = (0, -iu(t_1 - i3\beta/4)), \quad r_2 = (0, -iu(-i\beta/2)), \quad r_3 = (0, -iu(t_2 - i\beta/4)), \quad r_4 = (0, 0) \tag{51}$$

The normalized OTOC is then given by:

$$\begin{aligned} C(t_1, t_2) &= e^{\frac{K}{2}\sum_{i<j}(A_iA_jF_1(r_i-r_j))} = \exp\left(\frac{Kn^2}{2}W(t_1,t_2)\right), \\ W(t_1,t_2) &= -F(r_1-r_2) - F(r_1-r_3) + F(r_1-r_4) + F(r_2-r_3) - F(r_2-r_4) - F(r_3-r_4) \\ &= \frac{1}{2}\log\left[\frac{\sinh^2\left(\frac{\pi}{\beta}(t_1 - i3\beta/4)\right)\sinh^2\left(\frac{\pi}{\beta}(t_2 + i\beta/4)\right)}{\sinh^2\left(\frac{\pi}{\beta}(t_1 - i\beta/4)\right)\sinh^2\left(\frac{\pi}{\beta}(t_1 - t_2 - i\beta/2)\right)(-i)^2\sinh^2\left(\frac{\pi}{\beta}(t_2 - i\beta/4)\right)} \right] \end{aligned}$$

In the end, we obtain the following explicit form:

$$C(t_1, t_2) = \left[\frac{\cosh\left(\frac{\pi}{\beta}(t_1 - t_2)\right) - i\sinh\left(\frac{\pi}{\beta}(t_1 + t_2)\right)}{\left(\cosh\left(\frac{\pi}{\beta}(t_1 - t_2)\right) + i\sinh\left(\frac{\pi}{\beta}(t_1 + t_2)\right)\right)\cosh\left(\frac{\pi}{\beta}(t_1 - t_2)\right)} \right]^{2\Delta}$$

Based on these, we can now work out the corresponding Krylov metric. Being a CFT, the finite temperature auto-correlation function of the Luttinger liquids takes the same form as that of the SYK models. As a result, the operator wavefunction in the Krylov basis is identical to (23), and we have that:

$$\sum_{m,n}\varphi_m(t_1)\varphi_n(t_2)K_{mn}=F(t_1,t_2)=\cosh(\alpha t_{12})^{-2\Delta}\left(1-\left[\frac{\cosh(\alpha t_{12})-i\sinh(2\alpha T_{12})}{\cosh(\alpha t_{12})+i\sinh(2\alpha T_{12})}\right]^{2\Delta}\right). \tag{52}$$

where we have defined $\alpha=\pi/\beta, t_{12}=t_1-t_2, T_{12}=t_1+t_2$. The Krylov metric can therefore be computed by performing a similar double contour integral:

$$\begin{aligned} K_{mn} &= \delta_{mn}-D(m)^{-1}D(n)^{-1}\oint\frac{dy_1}{y_1^{m+1}}\oint\frac{dy_2}{y_2^{n+1}}\left[\frac{(1-iy_1)(1-iy_2)}{(1+iy_1)(1+iy_2)(1-y_1y_2)}\right]^{2\Delta} \\ &= \delta_{mn}-D(m)^{-1}D(n)^{-1}\int d\theta_1 d\theta_2\; e^{-S(\theta_1,\theta_2)} \end{aligned}$$

The effective action and saddle-point equation is given by:

$$\begin{aligned} S(\theta_1,\theta_2) &= m\theta_1+n\theta_2-2\Delta\log\left[\frac{\left(1-ie^{\theta_1}\right)\left(1-ie^{\theta_2}\right)}{(1+ie^{\theta_1})(1+ie^{\theta_2})(1-e^{\theta_1+\theta_2})}\right] \\ m+\frac{2i\Delta}{\cosh\theta_1}+\frac{2\Delta}{1-e^{-(\theta_1+\theta_2)}} &= 0,\quad n+\frac{2i\Delta}{\cosh\theta_2}+\frac{2\Delta}{1-e^{-(\theta_1+\theta_2)}}=0 \end{aligned} \tag{53}$$

These are high degree polynomial equations of $y_{1,2}=e^{\theta_{1,2}}$. In the limit of:

$$m=L(1-\lambda),\quad n=L(1+\lambda),\quad L\gg 1 \tag{54}$$

The dominant saddle-point can be obtained in series expansion of L^{-1}:

$$\begin{aligned} \theta_1^* &= -\frac{\pi i}{2}+\frac{2i\Delta}{1-\lambda}L^{-1}+O(L^{-2}) \\ \theta_2^* &= -\frac{\pi i}{2}+\frac{2i\Delta}{1+\lambda}L^{-1}+O(L^{-2}) \end{aligned} \tag{55}$$

Plugging this into the effective action, and neglecting the subdominant δ_{mn} term in K_{mn} then gives:

$$K_{mn}\sim(-1)^L L^{2\Delta+1}(1-\lambda^2)^{\Delta+1/2}\times(\text{fluctuation}) \tag{56}$$

Again, this result is matched well with the numerical result, for the diagonal part one can see the figures in maintext, for the off-diagonal, see FIG 3 (b). The alternating sign factor $(-1)^L$ comes from the imaginary leading order terms of $\theta_{1,2}^*$. The fluctuation part of the integral produces an additional factor $L^{-2}(1-\lambda^2)^{-1}$, which can be revealed by a similar analysis as before. We omit the details. Combining these factors we obtain that:

$$K_{mn}\sim(-1)^L L^{2\Delta-1}(1-\lambda^2)^{\Delta-1/2}=(-1)^{\frac{m+n}{2}}(mn)^{\Delta-1/2} \tag{57}$$

Example 3: MBL systems

The effective Hamiltonian for MBL systems takes the form:

$$H=\frac{1}{2}\sum_{i\neq j}J_{ij}\sigma_z^i\sigma_z^j+\sum_i h_i\sigma_z^i,\quad i,j\in[-N/2+1,N/2],\quad \text{with } N\to\infty \tag{58}$$

where the coefficients $\{J_{ij},h_i\}$ are independent Gaussian random variables with:

$$\langle J_{ij}\rangle=0,\quad\langle J_{ij}^2\rangle=J^2\exp\left(\frac{|i-j|}{\xi}\right),\quad\langle h_i\rangle=0,\quad\langle h_i^2\rangle=h^2 \tag{59}$$

We study the time evolution of the following operator localized at site $i=0$:

$$\sigma_x^0(t)=e^{iHt}\,\sigma_x^0\,e^{-iHt} \tag{60}$$

and construct the Krylov basis using the infinite temperature operator norm:

$$\langle A, B\rangle = \mathrm{Tr}\left(A^{\dagger}B\right) \tag{61}$$

The lanzcos coeffcients are then fixed by the infintie temperature auto-correlation function, which we now compute.

$$C(t) = \langle\sigma_x^0(t), \sigma_x^0(0)\rangle = \mathrm{Tr}\left(e^{iHt}\sigma_x^0 e^{-iHt}\sigma_x^0\right) = \mathrm{Tr}\left(\exp\left[2it\sum_{j\neq 0} J_{0j}\sigma_z^0\sigma_z^j + 2ith_0\sigma_z^0\right]\right)$$

where we have used that:

$$\sigma_x^0\sigma_z^j\sigma_x^0 = -\delta_{j0}\ \sigma_z^j\ \rightarrow \sigma_x^0\ e^{-iHt}\ \sigma_x^0 = e^{-iHt}\times\exp\left[2it\sum_{j\neq 0} J_{0j}\sigma_z^0\sigma_z^j + 2ith_0\sigma_z^0\right] \tag{62}$$

Applying the identity $e^{iJ\sigma_z} = \cos(J) + i\sin(J)\sigma_z$, the trace can be easily evaluated:

$$\begin{aligned} C(t) &= \mathrm{Tr}\prod_{j\neq 0}\left(\cos(2J_{0j}t) + i\sin(2J_{0j}t)\sigma_z^0\sigma_z^j\right)\left(\cos(2h_0t) + i\sin(2h_0t)\sigma_z^0\right) \\ &= \prod_{j\neq 0}\cos(2J_{0j}t)\cos(2h_0t) \end{aligned} \tag{63}$$

A more explicitly expression can be obtained by taking the statistical average:

$$\overline{C(t)} = \prod_{j\neq 0}\overline{\cos(2J_{0j}t)}\ \overline{\cos(2h_0t)} = e^{-\frac{\gamma^2}{2}t^2},\quad \gamma^2 = 4J^2\sum_{j\neq 0} e^{-|j|/\xi} + 4h^2 \tag{64}$$

We see that the auto-correlation function decays like a Gaussian, which happens to also be the case where the krylov basis wave-function and the Lanzcos coefficients are known explicitly: [48]:

$$C(t) = e^{-\frac{\gamma^2 t^2}{2}}\quad \rightarrow\quad \varphi_n(t) = e^{-\frac{\gamma^2 t^2}{2}}\frac{\gamma^n t^n}{\sqrt{n!}},\quad b_n = \gamma\sqrt{n} \tag{65}$$

In particular, for MBL systems the Lanzcos coefficients grow sub-linearly as $\sqrt{n}$. Notice that $\varphi_n(t)$ is also of the form that allows extracting the Krylov metric from the OTOC via explicit contour integrals. We start by considering:

$$\begin{aligned} F(t_1, t_2) &= -\frac{1}{N}\sum_m \mathrm{Tr}\left[\sigma_x^0(t_1), \sigma_x^m\right]\left[\sigma_x^0(t_2), \sigma_x^m\right] \\ &= 2C(t_{12}) - \frac{2}{N}\sum_m \mathrm{Tr}\left[\sigma_x^0(t_1)\ \sigma_x^m\ \sigma_x^0(t_2)\ \sigma_x^m\right] \end{aligned} \tag{66}$$

where N is total number of sites in the Hamiltonian. The OTOC term can be evaluated via similar tricks:

$$\begin{aligned} OTOC &= \sum_m \mathrm{Tr}\left[e^{iHt_1}\sigma_x^0 e^{-iHt_1}\ \sigma_x^m\ e^{iHt_2}\sigma_x^0 e^{-iHt_2}\ \sigma_x^m\right] \\ &= \sum_m \mathrm{Tr}\Big[e^{2it_1\sum_{j\neq 0}J_{0j}\sigma_z^0\sigma_z^j + 2it_1h_0\sigma_z^0}\ \sigma_x^0\sigma_x^m\ e^{2it_2\sum_{j\neq 0}J_{0j}\sigma_z^0\sigma_z^j + 2it_2h_0\sigma_z^0}\ \sigma_x^0\sigma_x^m\Big] \\ &= C(t_1+t_2) + \sum_{m\neq 0}\mathrm{Tr}\Big[e^{2it_1\sum_{j\neq 0}J_{0j}\sigma_z^0\sigma_z^j + 2it_1h_0\sigma_z^0}\sigma_x^m\ e^{-2it_2\sum_{j\neq 0}J_{0j}\sigma_z^0\sigma_z^j - 2it_2h_0\sigma_z^0}\ \sigma_x^m\Big] \\ &= C(t_1+t_2) + \sum_{m\neq 0}\cos(2J_{0m}(t_1+t_2))\prod_{j\neq 0,m}\cos\left(2J_{0j}t_{12}\right)\cos(2h_0(t_{12})) \end{aligned} \tag{67}$$

Taking the statistical average then gives:

$$\overline{F(t_1, t_2)} = 2e^{-\frac{\gamma^2}{2}t_{12}^2} - \frac{2}{N}e^{-\frac{\gamma^2}{2}(t_1+t_2)^2} - \frac{2}{N}\sum_{m\neq 0}\exp\left(-8J^2e^{-|m|/\xi}t_1t_2\right)e^{-\frac{\gamma^2}{2}\ t_{12}^2} \tag{68}$$

The explicit dependence on $\{t_1, t_2\}$ in (68) is complicated through the summation. In the late time limit $J^2 t_1 t_2/\xi \gg 1$, we can approximate the summation by replacing all those terms with small exponents, i.e. $8J^2 e^{-|m|/\xi} t_1 t_2 \leq 1$, by 1; and the others by 0. Doing this then gives:

$$\sum_{m\neq 0} \exp\left\{\left(-8J^2 e^{-|m|/\xi} t_1 t_2\right)\right\} \approx (N-1) - 2\xi \log\left(8J^2 t_1 t_2\right) \tag{69}$$

Plugging this back, we therefore obtain that:

$$\overline{F(t_1, t_2)} \approx \frac{2}{N} e^{-\frac{\gamma^2}{2}(t_1-t_2)^2} - \frac{2}{N} e^{-\frac{\gamma^2}{2}(t_1+t_2)^2} + \frac{2}{N}\xi \ln\left(8J^2 t_1 t_2\right) e^{-\frac{\gamma^2}{2}\,(t_1-t_2)^2} \tag{70}$$

Using the form of the operator wavefunction (65), the asymptotic Krylov metric is then related to $\overline{F(t_1, t_2)}$ at large t_1, t_2 via:

$$\sum_{m,n} t_1^m t_2^n K_{mn} = \frac{\sqrt{m!n!}}{\gamma^{m+n}} e^{\frac{\gamma^2}{2}(t_1^2+t_2^2)}\, \overline{F(t_1, t_2)} \approx \frac{2\sqrt{m!n!}}{N\gamma^{m+n}} \left(e^{\gamma^2 t_1 t_2} - e^{-\gamma^2 t_1 t_2} + 2\xi \ln\left(8J^2 t_1 t_2\right) e^{\gamma^2 t_1 t_2}\right) \tag{71}$$

The RHS only depends on the product $(t_1 t_2)$. As a consequence, the asymptotic Krylov metric is diagonal:

$$K_{mn} = K_{nn}\delta_{mn} \tag{72}$$

The diagonal elements can therefore be extracted by a single contour integral in $x = \gamma^2 t_1 t_2$:

$$K_n \approx \frac{2}{N} - \frac{2(-1)^n}{N} + \frac{2\xi n!}{N} \oint \frac{dx}{x^{n+1}} \ln\left(\frac{8J^2}{\gamma^2} x\right) e^x \tag{73}$$

At large order $n \gg 1$ the integral is approximated by the contribution from the dominant saddle-point x^* satisfying:

$$n + 1 = x^* + \ln\left(\frac{8J^2}{\gamma^2} x^*\right)^{-1} \to x^* \approx n \tag{74}$$

The fluctuation about the saddle gives an additional $\sqrt{n}$ factor. Combining these then gives the asymptotic behavior:

$$K_{nn} \approx \frac{2}{N} - \frac{2(-1)^n}{N} + \frac{2\xi}{N} \ln\left(\frac{8J^2}{\gamma^2} n\right) \approx \frac{2\xi}{N} \ln\left(\frac{8J^2}{\gamma^2} n\right) \tag{75}$$

SIZE-RESOLVED KRYLOV METRIC

The OTOCs can often be interpreted in terms of the operator-spreading under time-evolution. In models where the operator-size can be explicitly defined, one can construct eigen-states in the operator space with fixed operator-size:

$$\hat{N}|O_n\rangle = n|O_n\rangle \tag{76}$$

where $\hat{N}$ is the super-operator that measures the size of the operator states. For example, in the SYK models and the MBL systems the eigen-states of size n consists of:

$$|\chi_{i_1} \ldots \chi_{i_n}\rangle, \quad |\sigma^{i_1}_{\alpha_1} \ldots \sigma^{i_n}_{\alpha_n}\rangle, \quad \alpha_i \in \{x, y, z\} \tag{77}$$

In these models, $F(t_1, t_2)$ and the Krylov metric K_{mn} can be interpretted as the matrix elements of $\hat{N}$:

$$F(t_1, t_2) = \langle O(t_1)|\, \hat{N}\, |O(t_2)\rangle, \quad K_{mn} = \langle O_m|\, \hat{N}\, |O_n\rangle \tag{78}$$

We can probe more refined aspects of the Krylov metric by further resolving it into contributions from the operator space sectors, each of which contains operator states of only fixed sizes:

$$K_{mn} = \sum_{\ell} K_{mn}(\ell), \quad K_{mn}(\ell) = \langle O_m|\, \hat{N}\hat{P}(\ell)\, |O_n\rangle = \ell\, \hat{P}(\ell)_{mn} \tag{79}$$

where $\hat{P}$ is the super-projector into operator space with fixed operator size ℓ. The operator-size distribution $\hat{P}(\ell)_{mn}$ is equivalently encoded in the generating function, which is more accessible by explicit computation:

$$Z(t_1, t_2, \mu) = \langle O(t_1)|\, e^{-\mu\hat{N}}\, |O(t_2)\rangle = \sum_{\ell,m,n} e^{-\ell\mu} \hat{P}(\ell)_{mn}\, \varphi_m(t_1)\, \varphi_n(t_2)^* \tag{80}$$

Therefore, by computing the operator-size generating function $Z(t_1, t_2, \mu)$, we can retrieve the distribution $\hat{P}(\ell)_{mn}$ and hence the resolved Krylov metric $K_{mn}(\ell)$. In this section, we will perform this calculation for the examples where the operator-size can be explicitly defined, i.e. the SYK models and the MBL systems.

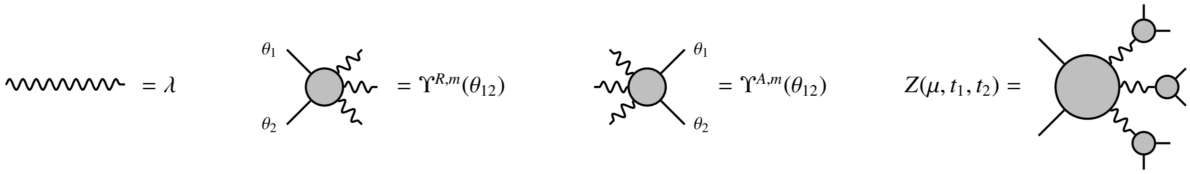

FIG. 4. A sketch of diagrammatics in the scramblon effective theory.

Example 1: the SYK models

We begin with the SYK models considered in the main text. Recall that these models contain N majorana fermions $\chi_i, i = 1, ..., N$ satisfying the anti-commutation relations:

$$\{\chi_i, \chi_j\} = 2\delta_{ij} \tag{81}$$

The generating function $Z(t_1, t_2, \mu)$ can be computed more conveniently by working in the doubled Hilbert-space $H_L \otimes H_R$. This allows us to defining the size super-operator explicitly as:

$$\hat{N} = \sum_i \frac{1}{2}\left(1 + i\chi_i^L \chi_i^R\right) \tag{82}$$

where χ_i^L and χ_i^R are majorana fermions acting on H_L and H_R respectively satsifying $\{\chi_i^L, \chi_j^R\} = 0$. To be compatible with this definition, the operator norm $\langle . \rangle$ is defined by the expectation value:

$$\langle \alpha, \beta \rangle = \langle I |\, \alpha_L^\dagger \beta_L \,| I \rangle = \mathrm{Tr}\left(\alpha^\dagger \beta\right) \tag{83}$$

in the maximally entangled state $|I\rangle$:

$$|I\rangle \propto \Pi_{i=1}^N c_i^\dagger \;|\Omega\rangle, \quad c_i = \frac{1}{2}\left(\chi_i^L - i\chi_i^R\right) \tag{84}$$

where $|\Omega\rangle = \Pi_{i=1}^N |\Omega\rangle_i^L \otimes |\Omega\rangle_i^R$ is the product state of the fermionic vacua for all $\chi_i^{L,R}$. The state $|I\rangle$ is chosen so that it is annihilated by the combination of fermion operators:

$$\left(\chi_i^L + i\chi_i^R\right)|I\rangle = 2c_i^\dagger |I\rangle = 0 \tag{85}$$

It is then easy to check that:

$$\hat{N}\,\chi_{i_1}^L ... \chi_{i_n}^L |I\rangle = n\,\chi_{i_1}^L ... \chi_{in}^L |I\rangle \tag{86}$$

and therefore fulfilling definition of the operator size operator. The definitions of the operator size can be extended to finite temperatures by replacing $|I\rangle$ by a thermal field double state $|TFD\rangle$:

$$|TFD\rangle \propto e^{-\frac{\beta}{4}(\hat{H}_L + \hat{H}_R)} |I\rangle \tag{87}$$

Analogous to before, in computing the norm using $|TFD\rangle$ we also separate the two operators by a $\rho^{1/2}$ insertion:

$$\begin{aligned} \langle \psi, \gamma_2 \rangle_{TFD} &= \langle I| e^{-\frac{\beta}{8}(\hat{H}_L + \hat{H}_R)} \psi_L^\dagger e^{-\frac{\beta}{4}\hat{H}_L} e^{-\frac{\beta}{4}\hat{H}_L} \gamma_L e^{-\frac{\beta}{8}(\hat{H}_L + \hat{H}_R)} |I\rangle \\ &= \mathrm{Tr}\left(\rho^{1/4}\psi^\dagger \rho^{1/2} \gamma \rho^{1/4}\right), \quad \rho = e^{-\beta \hat{H}} \end{aligned} \tag{88}$$

Alternatively this can can be understood as measuring the original operator size in the operator "smeared" by the thermal density matrix: $O \to \rho^{1/4} O \rho^{1/4}$.

It is very difficult to compute the generating function $Z(t_1, t_2, \mu)$ from first principles. Fortunately for the SKY models, progress can be made using the effective description based on the scramblon mode, see Figure (4). In this framework, the relevant dynamics can be captured by two ingredients: (i) the scramblon mode propagator λ, characterized by the lyapunov exponent $\varkappa$; (ii) the retarded/advanced vertex functions $\Upsilon^{R/A,m}(\theta_{12})$ describing the couplings to m scamblon modes, where $\theta_{ij} = \theta_i - \theta_j$ for the complexified time of insertion $\theta = \frac{2\pi}{\beta}(\tau + it)$. For our purpose, we can set $\Upsilon_m^R = \Upsilon_m^A = \Upsilon_m$ by assuming time-reflection symmetry. For more details please refer to [79]. The scramblon mode propagator λ is expected to take the universal form for generic lyapunov exponent $\varkappa$:

$$\lambda = -\frac{e^{i\frac{\varkappa}{2}(\pi+\theta_3+\theta_4-\theta_1-\theta_2)}}{C} \tag{89}$$

where C is a normalization constant proportional to N; while the explicit form of the vertex function $\Upsilon_m(\theta_{12})$ is less understood except at the maximal chaos $\varkappa = 1$, where it is explicitly given by:

$$\Upsilon^m(\theta_{12}) \;=\; \int_0^\infty dy\, y^m\, h(y,\theta_{12}),\quad h(y,\theta_{12}) = \frac{G}{\Gamma(2\Delta)}\, y^{2\Delta-1} e^{-\Theta_{12} y},\quad G = \frac{1}{2}\cos\left(\frac{\pi v}{2}\right)^{2\Delta},\quad \Theta_{12} = \cos\left[\frac{v(\pi-\theta_{12})}{2}\right] \tag{90}$$

where $\Delta = 1/q$ is the conformal dimension of χ in q-body SYK models, and v is given by:

$$\frac{\pi v}{\cos\left(\frac{\pi v}{2}\right)} = \beta J \tag{91}$$

For our purpose we will always focus on the strong coupling limit $v \to 1$. The OTOC can be expressed using these as:

$$OTOC = \sum_{m=0}^{\infty} \Upsilon^m(\theta_{12}) \frac{(\lambda)^m}{m!} \Upsilon^m(\theta_{34}) \tag{92}$$

The usual OTOC corresponds to setting:

$$\theta_1 = \frac{2\pi i}{\beta} t + \frac{\pi}{2},\quad \theta_2 = \frac{2\pi i}{\beta} t + \frac{3\pi}{2},\quad \theta_3 = \pi,\quad \theta_4 = 0 \tag{93}$$

For early time $t \ll \log N$, $\lambda \propto e^{\varkappa t}/N \ll 1$, and the OTOC is dominated by single scramblon exchange at $m = 1$, giving the exponential behavior in time. We are interested in computing the operator size generating function $Z(\mu, t_1, t_2)$ defined by:

$$\begin{aligned} Z(\mu,t_1,t_2) \;&=\; \left\langle \chi_1(t_1), e^{-\mu\hat{N}} \chi_1(t_2) \right\rangle_{TFD} \\ &=\; e^{-\frac{\mu N}{2}} \left\langle I \middle| e^{-\frac{\beta}{8}(\hat{H}_L+\hat{H}_R)} \chi_1^L(t_1) e^{-\frac{\beta}{4}\hat{H}_L} \sum_n \frac{1}{n!}\left(-\frac{i\mu}{2}\sum_i \chi_i^L\chi_i^R\right)^n \right. \\ &\times\; \left. e^{-\frac{\beta}{4}\hat{H}_L} \chi_1^L(t_2) e^{-\frac{\beta}{8}(\hat{H}_L+\hat{H}_R)} \middle| I \right\rangle \end{aligned} \tag{94}$$

We can again turn this expansion into correlation functions in terms of $\chi^L = \chi$ only. To this end, we need to shift χ_i^R in the size operator all the way to the left and use the identity (85) to transform it into χ_i^L. The key steps proceed as follows:

$$\begin{aligned} &\left(\sum_i \chi_i^L\chi_i^R\right)^n e^{-\frac{\beta}{4}\hat{H}_L} \chi_1^L(t_2) e^{-\frac{\beta}{8}(\hat{H}_L+\hat{H}_R)} \left| I \right\rangle \\ =\;& (-1)^{\frac{n(n-1)}{2}} \sum_{i_1,i_2,\ldots,i_n} \left(\chi_{i_1}^L \ldots \chi_{i_n}^L\right)\left(\chi_{i_n}^R \ldots \chi_{i_1}^R\right) e^{-\frac{\beta}{4}\hat{H}_L} \chi_1^L(t_2) e^{-\frac{\beta}{8}(\hat{H}_L+\hat{H}_R)} \left| I \right\rangle \\ =\;& (-1)^{\frac{n(n+1)}{2}} \sum_{i_1,i_2,\ldots,i_n} \left(\chi_{i_1}^L \ldots \chi_{i_n}^L\right) e^{-\frac{\beta}{4}\hat{H}_L} \chi_1^L(t_2) e^{-\frac{\beta}{8}\hat{H}_L} \left(\chi_{i_n}^R \ldots \chi_{i_1}^R\right) e^{-\frac{\beta}{8}\hat{H}_R} \left| I \right\rangle \\ =\;& (-i)^n \sum_{i_1,i_2,\ldots,i_n} \left(\chi_{i_1}^L \ldots \chi_{i_n}^L\right) e^{-\frac{\beta}{4}\hat{H}_L} \chi_1^L(t_2) e^{-\frac{\beta}{4}\hat{H}_L} \left(\chi_{i_1}^L \ldots \chi_{i_n}^L\right) \left| I \right\rangle \end{aligned} \tag{95}$$

where in the second last line we have used $\left(\hat{H}_R - \hat{H}_L\right)|I\rangle = 0$. Assemble everything, in the end we get the following expression:

$$\begin{aligned} Z(\mu,t_1,t_2) \;&=\; e^{-\frac{\mu N}{2}} \sum_n \frac{1}{n!} \left\langle \mathcal{T} \chi_1\left(t_1 + \frac{3i\beta}{4}\right)\left[-\frac{\mu}{2}\sum_i \chi_i\left(\frac{i\beta}{2}\right)\chi_i(0)\right]^n \right. \\ &\times\; \left. \chi_1\left(t_2 + \frac{i\beta}{4}\right)\right\rangle_\beta \end{aligned} \tag{96}$$

where $\langle\ldots\rangle = \mathrm{Tr}\,(\rho\ldots)$ is the thermal correlator and $\mathcal{T}$ denotes time-ordering in the imaginary time. This is a generalization of the OTOC. Through the effective model, this can be expressed in terms of $\Upsilon^{R/A,m}$ and λ:

$$Z(t_1,t_2,\mu) \;= e^{-\mu N\left(\frac{1}{2}-G(\theta_{34})\right)} \textstyle\sum_{m=0}^{\infty} \Upsilon^m(\theta_{12}) \left(\frac{\lambda\mu N}{2}\right)^m \frac{1}{m!} \Upsilon^1(\theta_{34})^m \tag{97}$$

It is worth making a few comments regarding (97): (i) we have included in the prefactor a factor of $e^{\mu N G(\theta_{34})}$ to factor out the disconnected contribution to the size operator $\hat{N}$ in the generating function, where the Green's function is given as:

$$G(\theta_{12}) = \frac{1}{2}\left[\frac{\cos\left(\frac{\pi v}{2}\right)}{\Theta_{12}}\right]^{2\Delta} \tag{98}$$

(ii) the vertex function insertions $\Upsilon^1(\theta_{34})$ related to the size operator only contains those associated with single scramblon emissions $m = 1$, this is the leading order contribution in the time regime $t \ll \log N$; (iii) the complexified time insertions are given explicitly by:

$$\theta_1 = \frac{2\pi i}{\beta}t_1 + \frac{\pi}{2}, \quad \theta_2 = \frac{2\pi i}{\beta}t_2 + \frac{3\pi}{2}, \quad \theta_3 = 0, \quad \theta_4 = \pi \tag{99}$$

To compute $Z(t_1, t_2, \mu)$ explicitly using (97) for generic $\varkappa$, we need the modification of the vertex function away from that of $\varkappa = 1$ given in (90). We can deduce this by examining how the structure of the OTOC is modified. At maximal chaos $\varkappa$ it can be written by plugging (90) into (92) as:

$$\begin{aligned} OTOC &= \int_0^\infty dy_1 \int_0^\infty dy_2 h(y_1, \theta_{12})\, h(y_2, \theta_{34})\, e^{-\lambda y_1 y_2} \\ &= \int_0^\infty dy_1 \int_0^\infty dy_2 h(y_1, \theta_{12})\, h(y_2, \theta_{34})\, e^{\frac{e^t}{C} y_1 y_2} \end{aligned} \tag{100}$$

where in the second line we have assigned $t_1 = t_2 = t,\ t_3 = t_4 = 0$ according to the usual OTOC conventions. The modifications to the OTOCs at submaximal chaos $\varkappa < 1$ has been studied, e.g. in contexts such as including the stringy corrections[9, 14]. The following form of modification was proposed:

$$\widetilde{OTOC} = \int_0^\infty dy_1 \int_0^\infty dy_2\ h(y_1, \theta_{12})\, h(y_2, \theta_{34})\, e^{\frac{e^{\varkappa t}}{C}(y_1 y_2)^{\varkappa}} \tag{101}$$

We shall assume that the form of modification can be extended to generic time insertions (t_1, t_2, t_3, t_4). Then we can absorb the modifications by re-writing:

$$\begin{aligned} \widetilde{OTOC} &= \int_0^\infty dy_1 \int_0^\infty dy_2\ \tilde{h}(y_1, \theta_{12})\, \tilde{h}(y_2, \theta_{34})\, e^{-\tilde{\lambda} y_1 y_2} \\ \tilde{\lambda} &= -\frac{e^{i\frac{\varkappa}{2}(\pi + \theta_3 + \theta_4 - \theta_1 - \theta_2)}}{C}, \quad \tilde{h}\left(y, \theta_{ij}\right) = \frac{y^{1/\varkappa - 1}}{\varkappa} h\left(y^{1/\varkappa}, \theta_{ij}\right) \end{aligned} \tag{102}$$

In other words, at submaximal chaos $\varkappa < 1$ we can work with the modified scramblon mode propagator $\tilde{\lambda}$, as well as the vertex function derived from the modified kernel $\tilde{h}$ in (102). In what follows, we shall use (102) to proceed with the computations for generic $\varkappa$. In terms of these, the generating function $Z(t_1, t_2, \mu)$ can be written as:

$$Z(t_1, t_2, \mu) = e^{-\mu N\left(\frac{1}{2} - G(\theta_{34})\right)} \int_0^\infty dy\ \tilde{h}(y, \theta_{12}) \exp\left(\frac{\tilde{\lambda}\mu N \Upsilon^1(\theta_{34})}{2} y\right) \tag{103}$$

For the insertions (99), the ingredients are given explicitly as follows:

$$\begin{aligned} \Theta_{12} &= \cosh\left(\frac{\pi t_{12}}{\beta}\right), \quad t_{12} = t_1 - t_2, \quad \Theta_{34} = 1 \\ \lambda &= -\frac{1}{C} e^{\frac{\pi\varkappa}{\beta}(t_1 + t_2)}, \quad \Upsilon^1(\theta_{34}) = \frac{\Gamma(2\Delta + \varkappa)}{\Gamma(2\Delta)} G, \quad G(\theta_{34}) = G \end{aligned} \tag{104}$$

Plugging these in, we obtain the following explicit form:

$$Z(t_1, t_2, \mu) = \frac{e^{-\mu N\left(\frac{1}{2} - G\right)} G}{\Gamma(2\Delta)} \int_0^\infty \frac{dy}{\varkappa}\, y^{\frac{2\Delta}{\varkappa} - 1} \exp\left[-\mu K e^{\frac{\varkappa\pi(t_1 + t_2)}{\beta}} y - \cosh\left(\frac{\pi t_{12}}{\beta}\right) y^{1/\varkappa}\right], \quad K = \frac{\Gamma(2\Delta + \varkappa)\mu N G}{2\Gamma(2\Delta) C} \tag{105}$$

We could now apply an inverse laplace transform and obtain:

$$\begin{aligned} P(t_1, t_2, \ell) &= \frac{1}{2\pi i} \oint_\Gamma d\mu\ e^{\mu \ell} Z(\mu, t_1, t_2) \\ &= \frac{G}{\Gamma(2\Delta)} \int_0^\infty \frac{dy}{\varkappa}\, \delta\left(\tilde{\ell} - K e^{\frac{\pi\varkappa}{\beta}(t_1 + t_2)} y\right)\, y^{\frac{2\Delta}{\varkappa} - 1} e^{-\cosh\left(\frac{\pi t_{12}}{\beta}\right) y^{1/\varkappa}} \\ &= \frac{G\, \tilde{\ell}^{2\Delta/\varkappa - 1}}{\varkappa K^{2\Delta/\varkappa} \Gamma(2\Delta)} \exp\left[-\frac{2\pi\Delta}{\beta}(t_1 + t_2) - \frac{1}{2}\left(\frac{\tilde{\ell}}{K}\right)^{1/\varkappa}\left(e^{-\frac{2\pi t_1}{\beta}} + e^{\frac{-2\pi t_2}{\beta}}\right)\right] \end{aligned} \tag{106}$$

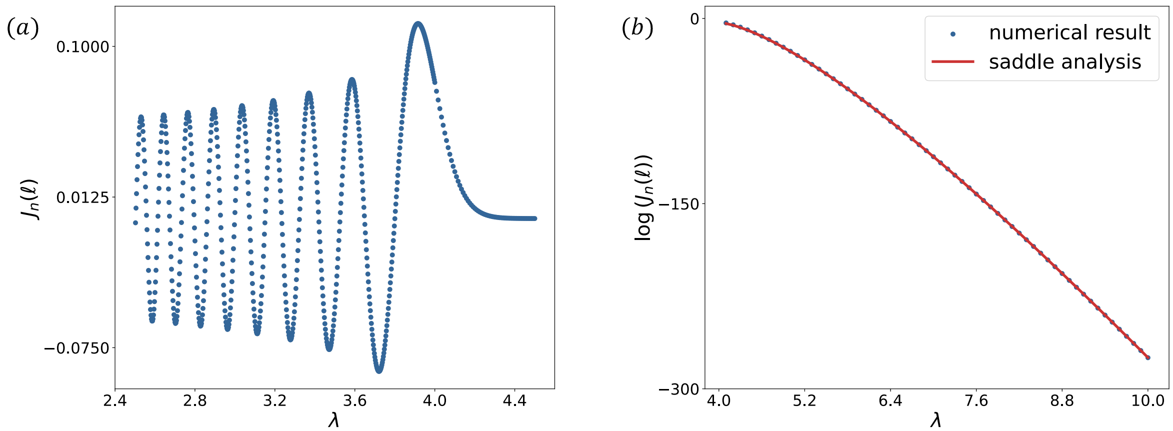

FIG. 5. We present the asymptotic behaviors of $J_n(\ell)$ as functions of $\lambda = \frac{(\ell/K)^{1/\varkappa}}{n}$ for $n = 150$: (a). the numerical result showing a transition between oscillatory and exponential decay across $\lambda = 4$; (b). the numerical result vs. saddle analysis in the exponential decay regime $\lambda > 4$.

where we have defined the renormalized operator-size $\tilde{\ell}$:

$$\tilde{\ell} = \ell - N\left(\frac{1}{2} - G\right) \tag{107}$$

We make some observations. Firstly the inverse laplace transform $P(t_1, t_2, \ell)$ depends on ℓ only through the combination $\left(\frac{\tilde{\ell}}{K}\right)^{1/\varkappa}$, which can be viewed as an effective operator-size for $\varkappa < 1$. Secondly, the dependence on the two time insertions $\{t_1, t_2\}$ of $P(t_1, t_2, \ell)$ can be factorized:

$$P(t_1, t_2, \ell) = Q_\ell(t_1) \times Q_\ell(t_2), \quad Q_\ell(t) = \frac{\tilde{\ell}^{\Delta/\varkappa - 1/2}}{\sqrt{\varkappa} K^{\Delta/\varkappa}} \sqrt{\frac{G}{\Gamma(2\Delta)}} e^{-\frac{2\pi\Delta}{\beta} t - \frac{1}{2}\left(\frac{\tilde{\ell}}{K}\right)^{1/\varkappa} e^{-\frac{2\pi}{\beta} t}} \tag{108}$$

As a consequence, $K_{mn}(\ell)$ also factorizes:

$$K_{mn}(\ell) = \ell J_m(\ell) J_n(\ell) \tag{109}$$

It is interesting to contemplate what is behind the observed factorization property of $K_{mn}(\ell)$. To see what is happening, let us write it as a product of rectangular matrices:

$$\ell^{-1} K_{mn}(\ell) = \left[L(\ell)^\dagger \cdot L(\ell)\right]_{mn} = J_m(\ell) J_n(\ell), \quad [L(\ell)]_{m\alpha} = \langle O_m, \alpha\rangle, \quad \alpha \in H_\ell \tag{110}$$

where H_ℓ denotes the operator space sector with fixed size ℓ. Factorization thus implies that the rectangular matrix $L(\ell)$ is of rank one. We can therefore deduce that:

$$\langle O_m, \alpha\rangle = [L(\ell)]_{m\alpha} = J_m(\ell) \times \Psi^\ell_\alpha \to \hat{P}(\ell)|O_m\rangle = J_m(\ell) \times |\Psi^\ell\rangle, \quad |\Psi^\ell\rangle = \sum_{\alpha \in \mathcal{H}_\ell} \Psi^\ell_\alpha |\alpha\rangle \tag{111}$$

In other words, distinct Krylov basis states O_m share the same normalized projection $|\Psi^\ell\rangle$ into each operator space sector H_ℓ. This is natural from the perspective that the Hamiltonian is symmetric under the permutation $P(n)$, the action of which is "ergodic" in each sector H_ℓ. We therefore expect the common projection $|\Psi^\ell\rangle$ to be the most permutation-symmetric operator state in H_ℓ. The factors $J_m(\ell)$ can therefore be viewed as the wave-function in operator-size of O_m.

In the case of $\varkappa = 1$, we can therefore compute $J_m(\ell)$ from $Q_\ell(t)$ via a single contour integral. Going through some algebra produces the following explicit integral:

$$J_n(\ell) = \frac{\tilde{\ell}^{\Delta/\varkappa - 1/2}}{\sqrt{\varkappa} K^{\Delta/\varkappa}} \sqrt{\frac{\Gamma(n+1) G}{\Gamma(2\Delta + n)}} \oint \frac{dy}{y^{n+1}} (1+y)^{-2\Delta} e^{-\frac{1}{2}\left(\frac{\tilde{\ell}}{K}\right)^{1/\varkappa}\left(\frac{1-y}{1+y}\right)} \tag{112}$$

To extract the global behavior of $J_n(\ell)$ at large n, it is appropriate to rescale $(\ell/K)^{1/\varkappa} = \lambda n$. The saddle-point equation and the solutions are then given by:

$$n + \frac{2\Delta y}{1+y} - \frac{\lambda n y}{(1+y)^2} = 0, \quad y^*_\pm = \frac{n(\lambda-2) - 2\Delta \pm \sqrt{(n\lambda - 2\Delta)^2 - 4n^2\lambda}}{2(n+2\Delta)} \tag{113}$$

It turns out that the physical saddle corresponds to y^*_-, while the other saddle y^*_+ gives a wave-function $J_n(\ell)$ that grows exponentially with ℓ. Now plugging this in and taking into account the scaling factor from the fluctuations, we obtain the following asymptotic behavior of $J_n(\tilde{\ell})$:

$$J_n(\tilde{\ell}) \sim \frac{\tilde{\ell}^{\Delta-1/2}}{K^\Delta}\sqrt{\frac{\Gamma(n+1)}{\Gamma(2\Delta+n)}}e^{-S^*} \times (\text{fluctuation}) \sim n^{-1/2}\left[e^{\frac{\sqrt{\lambda(\lambda-4)}}{2}}\left(\frac{\lambda - 2 - \sqrt{\lambda(\lambda-4)}}{2}\right)\right]^{-n} \tag{114}$$

This result is consistent with the numerical calculation for $\lambda > 4$, see FIG. 5 (b). From this, we see that the wave-function $J_n(\ell)$ exhibits a transition across $\lambda \sim 4$: in terms of the original renormalized operator size $\tilde{\ell}$, the wave-function is oscillatory in the regime: $\tilde{\ell} < K(4n)^\varkappa$; and decays exponentially in the regime: $\tilde{\ell} > K(4n)^\varkappa$, see FIG. 5 (a). As a result, one can estimate the typical operator size of O_n to be of order: $\tilde{\ell} \sim K n^\varkappa$.

Example 2: MBL systems

Next, let us consider the operator-size distribution of MBL systems. We begin with the Heisenberg evolution of σ^0_x. Applying the identity (62) introduced previously, we can derive:

$$\sigma^0_x(t) = e^{iHt}\sigma^0_x e^{-iHt} = \sigma^0_x \prod_{j\neq 0}\left(\cos(2J_{0j}t) + i\sin(2J_{0j}t)\sigma^0_z\sigma^j_z\right)\left(\cos(2h_0 t) + i\sin(2h_0 t)\sigma^0_z\right). \tag{115}$$

The generating function $Z(t_1, t_2, \mu)$ now is defined to be:

$$\begin{aligned} Z(t_1,t_2,\mu) &= \mathrm{Tr}\left[\sigma^0_x(t_1)e^{-\mu\hat{N}}\sigma^0_x(t_1)\right] \\ &= \mathrm{Tr}\Big\{\sigma^0_x \prod_{j\neq 0}\left(\cos(2J_{0j}t_1) + i\sin(2J_{0j}t_1)\sigma^0_z\sigma^j_z\right)\left(\cos(2h_0 t_1) + i\sin(2h_0 t_1)\sigma^0_z\right) \\ &\times\ e^{-\mu\hat{N}}\sigma^0_x \prod_{k\neq 0}\left(\cos(2J_{0k}t_2) + i\sin(2J_{0k}t_2)\sigma^0_z\sigma^k_z\right)\left(\cos(2h_0 t_2) + i\sin(2h_0 t_2)\sigma^0_z\right)\Big\} \end{aligned} \tag{116}$$

This can be computed by direct counting techniques. Let us study the pattern of Pauli strings that arise from taking products within either pf $\sigma^0_x(t_{1,2})$. The following observations arise: (i) each factor of $\cos(2J_{0j}t)$ corresponds to an identity operator on site j, while each factor of $\sin(2J_{0j}t)$ indicates the existence of a σ_z operator on site j; (ii) terms containing $\cos(2h_0 t)$ or $\sin(2h_0 t)$ differ by interchanging σ^0_x and σ^0_y. Taking trace then pairs up Pauli strings from $\sigma^0_x(t_{1,2})$. Therefore, We can neglect all cross terms between sine and cosine functions when computing the generating function, which gives:

$$Z(\mu,t_1,t_2) = e^{-\mu}\cos(2h_0(t_1-t_2))\prod_{j\neq 0}\left(\cos\left(2J_{0j}t_1\right)\cos\left(2J_{0j}t_2\right) + e^{-\mu}\sin(2J_{0j}t_1)\sin(2J_{0j}t_2)\right). \tag{117}$$

The first term $e^{-\mu}$ comes from the zeroth site, which is always occupied. Additional factor of $e^{-\mu}$ appears when other sites are occupied by σ_z. After taking the disorder average, it becomes

$$\begin{aligned} \overline{Z(\mu,t_1,t_2)} &= e^{-\mu}\overline{\cos(2h_0(t_1-t_2))}\prod_{j\neq 0}\left[\frac{1-e^{-\mu}}{2}\overline{\cos\left(2_{0j}(t_1+t_2)\right)} + \frac{1+e^{-\mu}}{2}\overline{\cos\left(2_{0j}(t_1-t_2)\right)}\right] \\ &= e^{-\mu}e^{-2h^2(t_1-t_2)^2}\prod_{j\neq 0}\left(\frac{1-e^{-\mu}}{2}e^{-2J^2(t_1+t_2)^2 e^{-\frac{|j|}{\xi}}} + \frac{1+e^{-\mu}}{2}e^{-2J^2(t_1-t_2)^2 e^{-\frac{|j|}{\xi}}}\right). \end{aligned} \tag{118}$$

Aiming at extracting K_{mn}, we multiply the generating function by $e^{\gamma^2(t_1^2+t_2^2)/2}$, with $\gamma^2 = 4J^2\sum_{j\neq 0}e^{-\frac{|j|}{\xi}} + 4h^2$ introduced previously. The result can be simplified as

$$\overline{Z(\mu,t_1,t_2)}e^{\frac{\gamma^2}{2}(t_1^2+t_2^2)} = e^{\gamma^2 t_1 t_2}e^{-\mu}\prod_{j\neq 0}\left(\frac{1+e^{-\mu}}{2} + \frac{1-e^{-\mu}}{2}e^{-8J^2 t_1 t_2 e^{-\frac{|j|}{\xi}}}\right). \tag{119}$$

Again, since this is only a function of $t_1 t_2$, we expect $K_{mn}(\ell)$ to be exactly diagonal for all ℓ. We can approximate the product via the similar logic used previously: when $8J^2 t_1 t_2 e^{-\frac{|j|}{\xi}} \gg 1$, the bracket gives $(1+e^{-\mu})/2$, indicating an equal probability between σ_z^j and I; for $8J^2 t_1 t_2 e^{-\frac{|j|}{\xi}} \ll 1$, the bracket is 1, which indicates a trivial identity operator. Under this approximation, we have that:

$$\overline{Z(\mu, t_1, t_2)} e^{\frac{\gamma^2}{2}(t_1^2+t_2^2)} \approx e^{\gamma^2 t_1 t_2} e^{-\mu} \left(\frac{1+e^{-\mu}}{2}\right)^{2\xi \ln\left(8J^2 t_1 t_2\right)} = e^{\gamma^2 t_1 t_2} 2^{-M(t_1 t_2)} \sum_{\ell} B\left(M(t_1 t_2), \ell\right) e^{-\mu(\ell+1)} = \sum_{\ell} e^{-\mu \ell} \ell^{-1} \sum_{n} \frac{(\gamma^2 t_1 t_2)^n}{n!} K_{nn}(\ell) \tag{120}$$

where $M(t_1 t_2) = 2\xi \ln\left(8J^2 t_1 t_2\right)$ and $B(M, \ell)$ is the binomial coefficient. The resolution $K_n n(\ell)$ of the diagonal Krylov metric into fixed operator-size ℓ can therefore be written in $x = \gamma^2 t_1 t_2$ as:

$$K_{nn}(\ell) \approx \frac{n!\ell}{2\pi i} \oint \frac{dx}{x^{n+1}} \left[\frac{B\left(M(x/\gamma^2), \ell - 1\right)}{2^{M(x/\gamma^2)}}\right] e^x \tag{121}$$

For M, ℓ both large and of the same order, the binomial coefficients approaches a Gaussian distribution:

$$\frac{B(M, \ell)}{2^M} \approx (\pi M/2)^{-1/2} e^{-\frac{(\ell - M/2)^2}{M/2}} \tag{122}$$

Giving the following integral expression that allows the saddle-point approximation:

$$K(\ell) \approx \frac{n!\ell}{2\pi i} \oint dx \ \exp\left(-(n+1)\ln x + x - \frac{\left(\ell - \xi \ln\left(\frac{8J^2}{\gamma^2} x\right)\right)^2}{\xi \ln\left(\frac{8J^2}{\gamma^2} x\right)} - \frac{1}{2} \ln\left(\pi \xi \ln\left(\frac{8J^2}{\gamma^2} x\right)\right)\right) \tag{123}$$

To access the global distribution, we can rescale $\ell = \lambda \ln n$. The dominant saddle-point solutions in this limit is simply:

$$x^* = n + .. \tag{124}$$

Plugging this back into the integral and taking care of the additional factor from the fluctuations, we obtain in the end the asymptotic form:

$$K_{nn}(\ell) \sim \lambda \exp\left(-\frac{(\lambda - \xi)^2}{\xi} \ln n\right) \tag{125}$$

We end with a few comments. The operator-size distribution of O_n is given by a Gaussian with the average size:

$$\bar{\ell} \sim \xi \ln n \tag{126}$$

It is also worth understanding the diagonal property of $K_{mn}(\ell)$ for any ℓ. In particular, it implies that:

$$K_{mn}(\ell) = \ell \langle O_m | \, \hat{P}(\ell) \, | O_n \rangle = \ell \langle \hat{P}(\ell) O_m, \hat{P}(\ell) O_n \rangle \propto \delta_{mn} \tag{127}$$

In other words, distinct Krylov basis elements project onto mutually orthogonal states in each sector H_ℓ. This reflects the localized nature of the dynamics as it explores within each sector of the operator space with fixed size ℓ.